AD-A032 073 MICHIGAN TECHNOLOGICAL UNIV HOUGHTON F/G 11/6
INTERFACIAL STRUCTURE, GROWTH KINETICS AND MECHANISMS OF THE PR--ETC(U)
OCT 76 H I AARONSON, J M RIGSBEE, J R BRADLEY DA-AROD-31-124-73-G144
UNCLASSIFIED ARO-11264.17-MC NL

1 OF 1
ADA032073

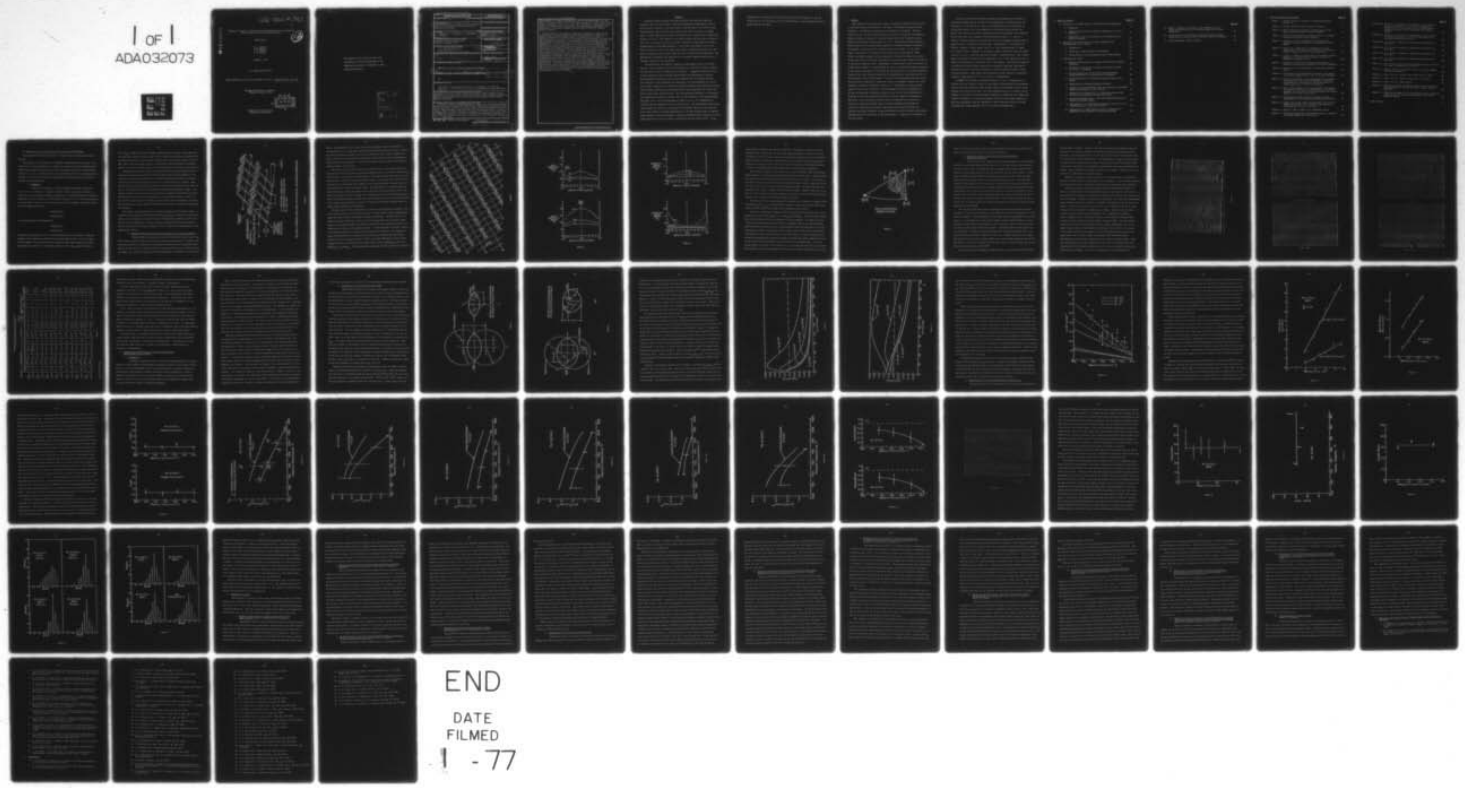

END

DATE
FILMED
1 -77

Interfacial Structure, Growth Kinetics and Mechanisms of the Proeutectoid Ferrite Reaction in Fe-C and Fe-C-X Alloys

(12)

Final Report

H. I. Aaronson
J. M. Rigsbee
J. R. Bradley
G. J. Shiflet

October 7, 1976

U. S. Army Research Office

Grants DA-AROD-31-124-73-G144 and DAHC04 75 G 0154: 18 March 1973-15 July 1976

Michigan Technological University
Houghton, Michigan 49931

1473

The findings in this report are not to be construed as an official Department of the Army position, unless so designated by other authorized documents.

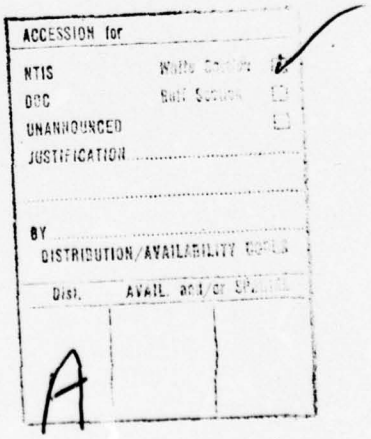

SECURITY CLASSIFICATION OF THIS PAGE (When Data Entered)

REPORT DOCUMENTATION PAGE

READ INSTRUCTIONS BEFORE COMPLETING FORM

1. REPORT NUMBER: 17
2. GOVT ACCESSION NO.:
3. RECIPIENT'S CATALOG NUMBER:

4. TITLE (and Subtitle): Interfacial Structure, Growth Kinetics and Mechanisms of the Proeutectoid Ferrite Reaction in Fe-C and Fe-C-X Alloys.

5. TYPE OF REPORT & PERIOD COVERED:

6. PERFORMING ORG. REPORT NUMBER:

7. AUTHOR(s): H. I. Aaronson, J. M. Rigsbee, J. R. Bradley, G. J. Shiflet

8. CONTRACT OR GRANT NUMBER(s): DA-ARO-D-31-124-73-G144; DAHC04-75-G-0154

9. PERFORMING ORGANIZATION NAME AND ADDRESS: Michigan Technological University, Houghton, Michigan 49931

10. PROGRAM ELEMENT, PROJECT, TASK AREA & WORK UNIT NUMBERS: 12 71 P.

11. CONTROLLING OFFICE NAME AND ADDRESS: U. S. Army Research Office, Post Office Box 12211, Research Triangle Park, NC 27709

12. REPORT DATE: October 4, 1976

13. NUMBER OF PAGES: 71

14. MONITORING AGENCY NAME & ADDRESS (if different from Controlling Office): 18 ARO 19 11264.17-MC

15. SECURITY CLASS. (of this report): Unclassified

15a. DECLASSIFICATION/DOWNGRADING SCHEDULE: NA

16. DISTRIBUTION STATEMENT (of this Report):

Approved for public release; distribution unlimited.

9 Rept. no. 17 (Final), 18 Mar 73 - 15 Jul 76

17. DISTRIBUTION STATEMENT (of the abstract entered in Block 20, if different from Report):

NA

18. SUPPLEMENTARY NOTES:

The findings in this report are not to be construed as an official Department of the Army position, unless so designated by other authorized documents.

19. KEY WORDS (Continue on reverse side if necessary and identify by block number):
interfacial structure; ledges; misfit dislocations; growth kinetics; growth mechanisms; solute drag effect; diffusional growth; shear; proeutectoid ferrite; massive transformation; Fe-C; Fe-C-X; Cu-Zn; Cu-Cr; AuCuII; surface relief effects; stereology

20. ABSTRACT (Continue on reverse side if necessary and identify by block number):
Two major research programs and numerous smaller ones have been completed during the tenure of these grants. One major program was an experimental study of the interfacial structure of the broad faces of ferrite plates in an Fe-C-Si alloy. Using weak-beam, dark-field TEM, this structure was shown to consist of a single array of misfit dislocations, spaced 15-25 Å apart, and a single array of ledges with spacings of 22-44 Å. The ledges are invariably triatomic and they cause the apparent habit plane to deviate from $\{111\}_\gamma$ by 9-18°; orientation

over

DD FORM 1 JAN 73 1473 EDITION OF 1 NOV 65 IS OBSOLETE

Unclassified

SECURITY CLASSIFICATION OF THIS PAGE (When Data Entered)

228 570

relationships lie between Kurdjumow-Sachs and Nishiyama-Wasserman. In all cases, the Burgers vector of the misfit dislocations lies in the atomic habit planes, invariably $\{110\}_\alpha // \{111\}_\gamma$, and hence thickening of these ferrite plates by shear is mechanistically impossible. The experimental investigation was supported by a concurrent computer modeling study of partially coherent fcc:bcc interfaces.

The second major investigation comprised an experimental study of the growth kinetics of grain boundary ferrite allotriomorphs as a function of reaction temperature and carbon content in high-purity Fe-C alloys. A supporting theoretical study of the stereology of grain boundary allotriomorphs was simultaneously conducted. The experimental study showed that at small undercoolings the measure parabolic rate constants for the thickening and lengthening of the allotriomorphs are as much as an order of magnitude less than those calculated assuming carbon diffusion-control; with increased undercooling, the measured growth rates approached more closely, but did not quite reach those calculated. This discrepancy was ascribed to the presence of a proportion of partially coherent facets at the boundaries of the allotriomorphs. The aspect ratio of the allotriomorphs was found to be ca. 1/3, independently of reaction time and temperature and also carbon content. The accompanying stereological study examined the effects of sectioning and allotriomorph above its center and also at an angle normal to the plane perpendicular to the grain boundary upon the apparent growth kinetics of the allotriomorph. Important differences between apparent and true growth kinetics were found to result, particularly from the latter factor. It was concluded that the experimental method used during this investigation is the most satisfactory one for determining the true growth kinetics of grain boundary allotriomorphs presently available.

Abstract

Two major research programs and numerous smaller ones have been completed during the tenure of these grants. One major program was an experimental study of the interfacial structure of the broad faces of ferrite plates in an Fe-C-Si alloy. Using weak-beam, dark-field TEM, this structure was shown to consist of a single array of misfit dislocations, spaced 15-25 Å apart, and a single array of ledges with spacings of 22-44 Å. The ledges are invariably triatomic and they cause the apparent habit plane to deviate from $\{111\}_\gamma$ by 9-18°; orientation relationships lie between Kurdjumow-Sachs and Nishiyama-Wasserman. In all cases, the Burgers vector of the misfit dislocations lies in the atomic habit planes, invariably $\{110\}_\alpha // \{111\}_\gamma$, and hence thickening of these ferrite plates by shear is mechanistically impossible. The experimental investigation was supported by a concurrent computer modeling study of partially coherent fcc:bcc interfaces.

The second major investigation comprised an experimental study of the growth kinetics of grain boundary ferrite allotriomorphs as a function of reaction temperature and carbon content in high-purity Fe-C alloys. A supporting theoretical study of the stereology of grain boundary allotriomorphs was simultaneously conducted. The experimental study showed that at small undercoolings the measured parabolic rate constants for the thickening and lengtheing of the allotriomorphs are as much as an order of magnitude less than those calculated assuming carbon diffusion-control; with increased undercooling, the measured growth rates approached more closely, but did not quite reach those calculated. This discrepancy was ascribed to the presence of a proportion of partially coherent facets at the boundaries of the allotriomorphs. The aspect ratio of the allotriomorphs was found to be ca. 1/3, independently of reaction time and temperature and also carbon content. The accompanying stereological study examined the effects of sectioning an allotriomorph above its center and also at an angle normal to the plane perpendicular to the grain boundary upon the apparent growth kinetics of the allotriomorph. Important differences between apparent and true growth kinetics were found to result, particularly from the latter factor. It was

concluded that the experimental method used during this investigation is the most satisfactory one for determining the true growth kinetics of grain boundary allotriomorphs presently available.

1. Forward

This program has been primarily a study of interphase boundaries and their role in diffusional phase transformations. Two types of interphase boundary have been considered: the partially coherent and the disordered or incoherent. When the crystal structure of the precipitate differs from that of the matrix, the partially coherent boundary is expected to interfere significantly with the growth process whereas the disordered boundary should not (1,2). The partially coherent boundary should migrate by the ledge mechanism whereas the disordered boundary is expected to be displaced by continuous atomic transfer across the boundary. At the present stage of development of transmission electron microscopy (excluding the highly refined instruments employed only by specialists), the misfit dislocation structure of partially coherent boundaries can usually be resolved by TEM, whereas the structure of disordered boundaries cannot. Measurements of growth kinetics have thus become the primary means available for understanding the nature of disorderd interphase boundaries. In the present investigation, the migrational characteristics of disordered interphase boundaries have been studied by measuring the lengthening and thickening kinetics of grain boundary ferrite allotriomorphs. The choice of allotriomorphs was made because this precipitate morphology is considered to have an interphase boundary with a predominantly disordered interfacial structure (1). (The presence of some partially coherent facets at the interfaces of allotriomorphs has long been recognized (1), but the allotriomorphic morphology remains the only one in an as-transformed microstructure in which the disordered interfacial structure appears to predominate.) The choice of the proeutectoid ferrite reaction in high-purity Fe-C alloys as a vehicle for studying the growth kinetics of grain boundary allotriomorphs was dictated in large part by the unique completeness and accuracy with which the necessary ancillary information on phase boundaries (and their metastable equilibrium extrapolations) and diffusivity in the matrix phase vs. composition is available in the Fe-C system.

In the case of partially coherent boundaries, much progress has been made in resolving and explaining the structure of such boundaries at interfaces which are "obviously" of this type (2,3). That is, the matching across such boundaries is clearly good enough so that the boundaries can be rendered fully coherent over most of their area by the periodic insertion of misfit dislocations in the boundary. On the other hand, even optimally fitting interfaces between f.c.c. and b.c.c. crystals probably represent the prototypical case of an interphase boundary which is not obviously of the partially coherent type. Morphological (1) and kinetic (2) evidence, however, strongly suggest that it is. And a modeling study (6) opened up a different type of approach to interphase boundary construction which can render certain f.c.c.:b.c.c interfaces partially coherent. Another portion of this investigation was devoted to making a direct experimental test of this approach and also to further strengthening the theoretical base of the approach. The study was conducted on proeutectoid ferrite plates, despite the considerable additional experimental difficulty involved in achieving retention of sufficient austenite matrix to make the study feasible, simply because the proeutectoid ferrite reaction is universally accepted as the prototype of an f.c.c.-to-b.c.c. transformation.

A summary of the study on partially coherent f.c.c.:b.c.c. boundaries constitutes the first technical section of this report; a description of the investigation on the growth kinetics of grain boundary ferrite allotriomorphs in Fe-C alloys provides the s-cond such section. The final technical section is a series of brief summaries of a number of shorter programs undertaken in preparation for, support and further development of the two main programs, and also of some longer programs for which the experimental work was undertaken at other laboratories with the writeup for publication being completed in part or in whole at Michigan Tech.

2. Table of Contents

3. List of Illustrations and Tables

A. The Structure of the Broad Faces of Proeutectoid Ferrite Plates

This program is being executed by Dr. J. Michael Rigsbee, postdocotral research associate.

The purposes of this program are to determine experimentally the structure of the broad faces of ferrite sideplates, to compare this structure with that deduced by Hall, Aaronson and Kinsman (6) and by Russell, Hall, Kinsman and Aaronson (7) for partially coherent f.c.c.:b.c.c. boundaries and to ascertain whether or not it is mechanistically possible for a ferrite plate with the experimentally observed interfacial structure to thicken by a shear mechanism.

1. Background

Brooks (4) and Paxton (5) have concluded that mismatch between the f.c.c. and b.c.c. lattices is too great to permit a misfit dislocation structure to exist even at a particularly favorable orientation of a boundary between these lattices. During the course of studies on the interfacial structure of b.c.c. Cr-rich precipitates in a Cu-Cr matrix, Hall et al (6) pointed out that at the interphase boundaries defined by the Kurdjumow and Sach (20)

$$\{110\}_\alpha // \{111\}_\gamma$$

$$\langle 111\rangle_\alpha // \langle 110\rangle_\gamma$$

or by the Nishiyama (20)-Wasserman (22)

$$\{110\}_\alpha // \{111\}_\gamma$$

$$\langle 110\rangle_\alpha // \langle 211\rangle_\gamma$$

orientation relationships, only ca. 8% of the atoms in one of the planes forming the boundary can be regarded as coherent with the atoms opposite them in the other plane of the boundary. The coherent atoms are grouped in small regions whose size, shape and spacing are sensitive to the precise rotation of the $\{111\}_{fcc}$ plane relative to

the $\{110\}_{bcc}$ plane in the 5-1/4° rotation range between K-S and N-W. They found that by inserting a monatomic ledge between coherent regions these regions are repeated and are shifted laterally. In this manner, the proportion of coherency could be raised to 25%. Hall et al were unable, however, to achieve the resolution needed to ascertain whether or not the monatomic ledges were actually present on their Cr-rich precipitates.

Subsequently, Russell et al (2), concerned about the mechanism through which the supposedly disordered areas between coherent regions would restrain migration of the interphase boundaries, recognized that in the N-W case each disordered area actually contains just one more atom per row in the f.c.c. than in the b.c.c. lattice. Thus, the presence of a misfit dislocation along the center of each disordered area would result in a classical dislocation interphase boundary, with the monatomic ledges -- now termed structural ledges because they serve only to complete the interfacial structure and cannot participate in the growth process -- being an added feature. Figure 1 is an isometric sketch of such an interface prepared during this investigation, illustrating the structural ledges, sample coherent areas and two misfit dislocations orthogonal to the ledges.

The efforts made to extend and to test these concepts have followed two paths. A computer modeling study of the structure of $\{110\}_{bcc}/\{111\}_{fcc}$ interfaces has been undertaken, and a transmission electron microscopic investigation is underway on the broad faces of ferrite sideplates. Since the computer modeling work has been completed, it will be summarized first; these findings will then be used in the interpretation of the experimental studies.

2. Computer Modeling Study of Partially Coherent F.c.c.:B.c.c. Boundaries

These studies were conducted at about 120 different rotation angles from N-W to K-S and beyond and for a wide range of lattice parameter ratios. For each interface, atom matching was computed for the atom pairs produced by all six possible combinations of the three f.c.c. planes parallel to $\{111\}_{\gamma}$ and the two b.c.c. planes parallel to $\{110\}_{\alpha}$. This involved calculation of atom matching for ca. 50,000 f.c.c.:b.c.c. atom

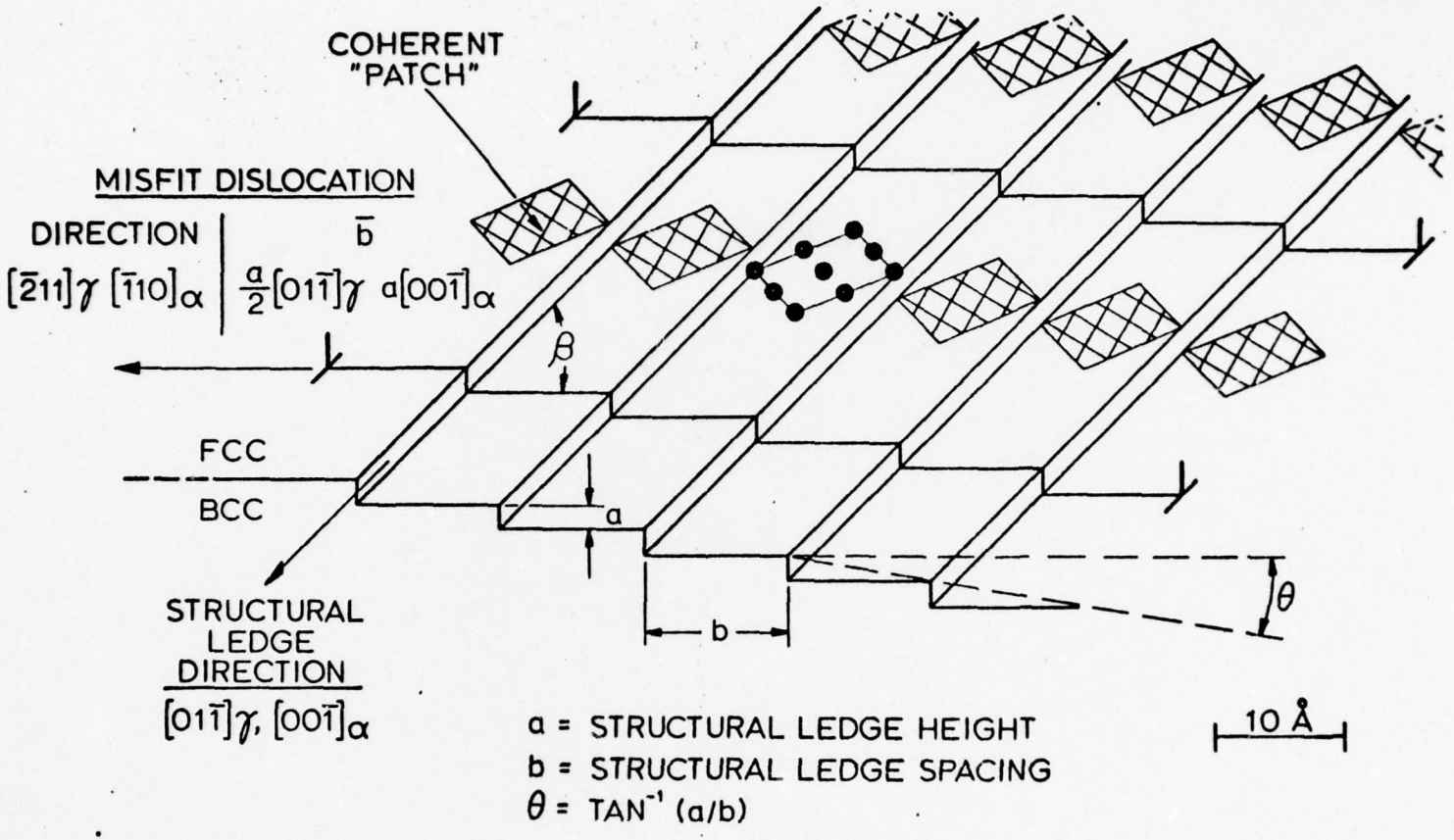

FCC: BCC INTERFACE STRUCTURE FOR NISHIYAMA - WASSERMAN ORIENTATION

Figure 1

pairs. Following Hall et al, a pair of atoms is considered to match coherently if translating the f.c.c. atom into a position exactly matching that of its b.c.c. counterpart does not involve movement over more than 15% of the f.c.c. nearest neighbor distance. Choice of a more restrictive definition of coherency has little fundamental effect upon the results reported. On the 15% definition, coherent regions were found to contain between 7 and 50 atoms.

The position, spacing and direction of possible arrays of structural ledges were determined, and then the position, spacing and Burgers vector of the misfit dislocations were evaluated. As expected, the organization of the misfit dislocation structure is dependent upon the array of structural ledges selected. The Burgers vector of the misfit dislocations was determined with a Burgers circuit through adjacent coherent regions of the broad face of a single structural ledge. The combination of structural ledge and misfit dislocation arrays was sought for each rotation of the two lattices which would yield the minimum interfacial energy. This condition was fulfilled by selecting interfaces with maximum coherency and with the smallest Burgers vector of misfit dislocations. It was found that programming to choose the interface with the most closely spaced coherent regions fulfilled both conditons.

The key result of this investigation is that for every rotational orientation and every lattice parameter ratio studied, at least one (and usually several energetically equal) partially coherent interfacial structure is predicted. Virtually all of the partially coherent boundaries contain both misfit dislocations and structural ledges. Figure 2 is a typical computed structure and shows both sets of defects as well as the locations of the atoms in the coherent regions. At each interface, the misfit dislocation structure consists of a single array of parallel dislocations. The spacing between the dislocations is a function of the rotational orientation and the lattice parameter ratio, and ranges from 8.6 to 40 Å. The misfit dislocations at the lowest energy interfaces always have a lattice-type Burgers vector, $\underline{a}/2\langle 110\rangle_{fcc}$ and either $\underline{a}/2\langle 111\rangle_{bcc}$ or $\underline{a}\langle 100\rangle_{bcc}$. The dislocations are usually of mixed type but are occasion-

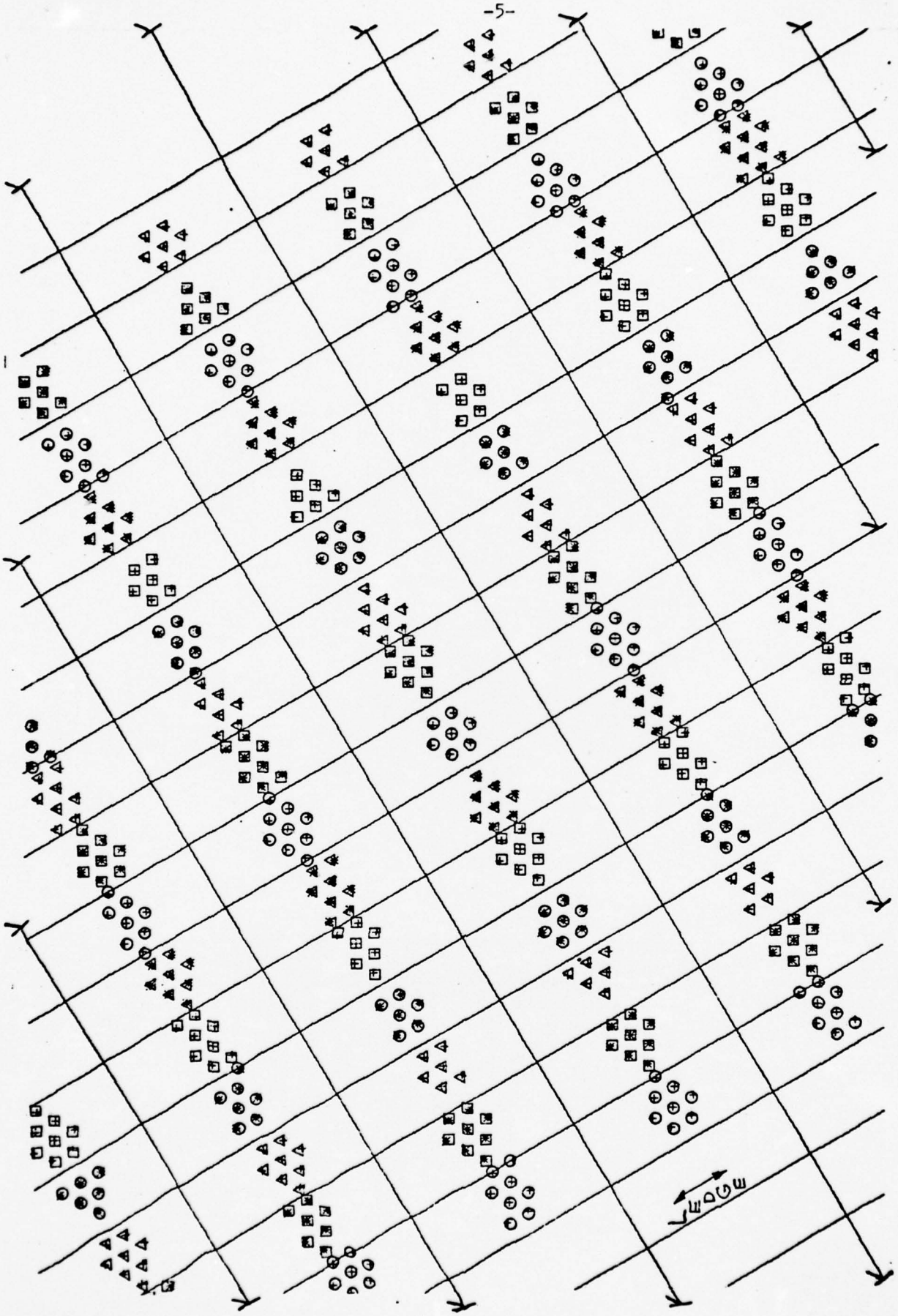

Figure 2

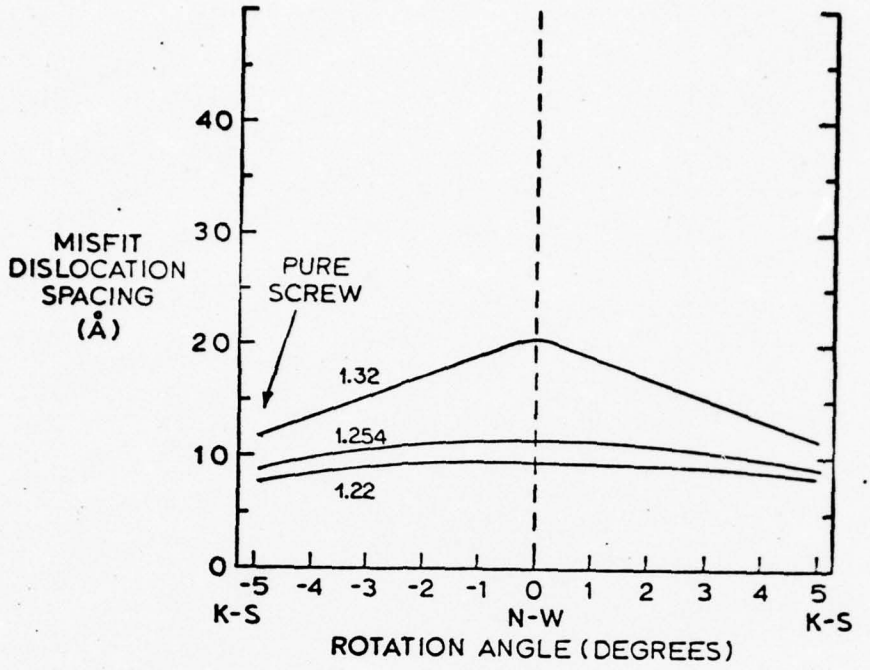
MISFIT
DISLOCATION
SPACING
(Å)
PURE
SCREW
1.32
1.254
1.22
40
30
20
10
0
-5 -4 -3 -2 -1 0 1 2 3 4 5
K-S
N-W
K-S
ROTATION ANGLE (DEGREES)

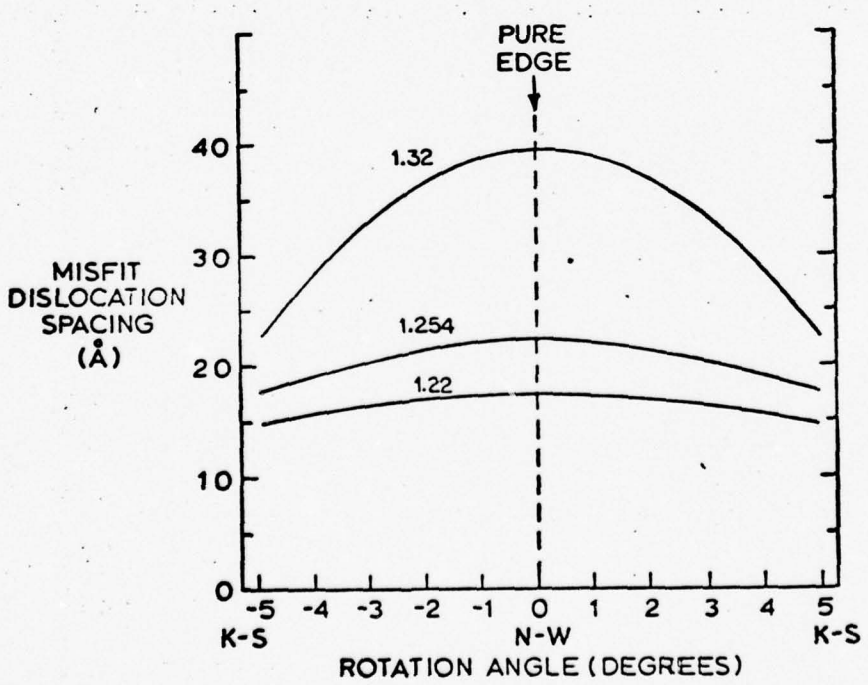
PURE
EDGE
1.32
1.254
1.22
MISFIT
DISLOCATION
SPACING
(Å)
40
30
20
10
0
-5 -4 -3 -2 -1 0 1 2 3 4 5
K-S
N-W
K-S
ROTATION ANGLE (DEGREES)

Figure 3

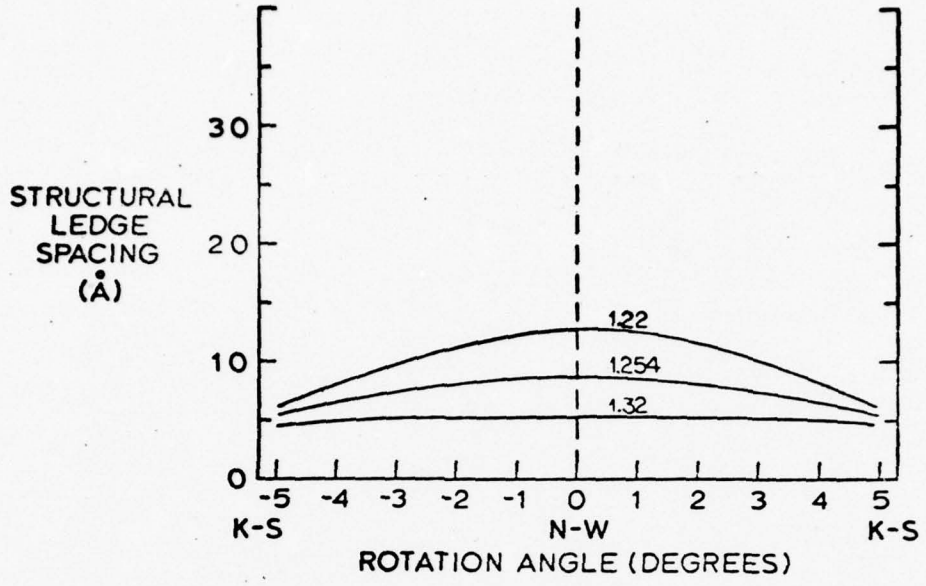
STRUCTURAL
LEDGE
SPACING
(Å)
30
20
10
0
1.22
1.254
1.32
-5 -4 -3 -2 -1 0 1 2 3 4 5
K-S
N-W
K-S
ROTATION ANGLE (DEGREES)

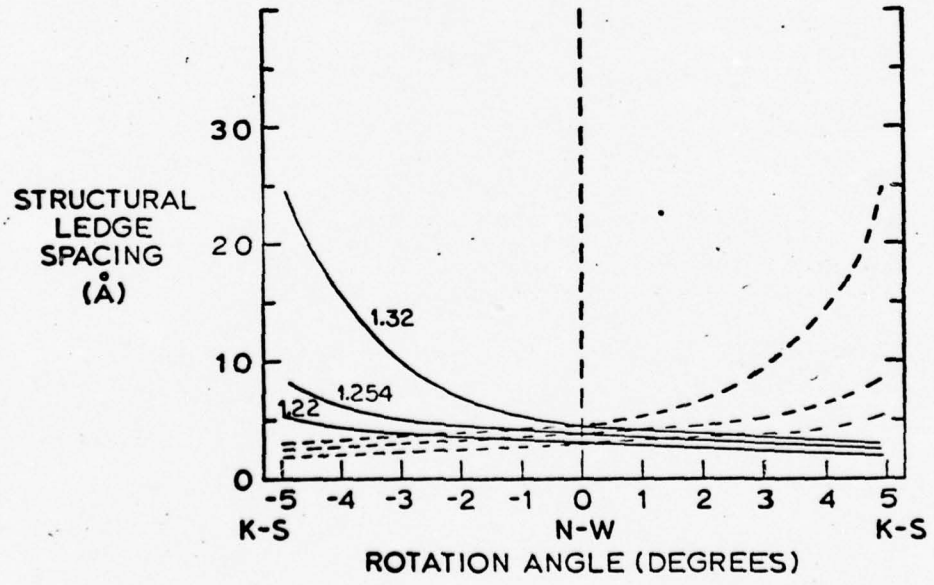
STRUCTURAL
LEDGE
SPACING
(Å)
30
20
10
0
1.32
1.254
1.22
-5 -4 -3 -2 -1 0 1 2 3 4 5
K-S
N-W
K-S
ROTATION ANGLE (DEGREES)

Figure 4

ally either pure edge or pure screw in character. Two types of equally low energy boundary can be constructed. At one, a pure edge dislocation is present at the N-W orientation, and at the other a pure screw dislocation obtains at the K-S orientation. Figure 3 shows the effects of rotation angle upon the misfit dislocation spacing at three lattice parameter ratios for the two types of structure. The former structure is seen to be characterized by appreciably larger inter-dislocation spacings.

The structural ledges are also present as a single, parallel array, with spacing again dependent on rotational orientation and lattice parameter ratio. When the ledges are monatomic, the spacing between ledges varies from ca. 3 to 30 Å. In some cases, structural ledges more than one atom plane high were found to yield a larger proportion of coherent regions (and hence a lower interfacial energy). In such situations, the spacing between ledges is simply increased proportionately. Figure 4 shows the influence of rotation angle and lattice parameter ratio upon the spacing between structural ledges in the two types of interphase boundary structure.

The structural ledges cause substantial deviations of the apparent conjugate habit from $\{110\}_{bcc}//\{111\}_{fcc}$. As illustrated in Figure 5, almost any apparent habit plane within the (110)-(211)-(111) region can be explained in this manner.

In all cases examined, the Burgers vector of the misfit dislocations lies in the plane of the atomic habit planes, i.e., $\{110\}_{bcc}$ and $\{111\}_{fcc}$. Hence one must conclude that these boundaries cannot be displaced by a shear mechanism. As noted in section II-E-8, the experimental studies of Watson and McDougall (23) on the crystallography proeutectoid ferrite plates are not in good agreement with the predictions of the phenomenological theory of martensite, and the surface relief effect which they measured corresponds to a shear much too large to make the formation of ferrite plates by this mechanism thermodynamically feasible throughout virtually the entire temperature-composition region of the proeutectoid ferrite reaction in Fe-C alloys (24). As is discussed further in section II-E-7, however, it seems likely that even when a precipitate plate exhibits both crystallography and surface relief effects consistent with the dic-

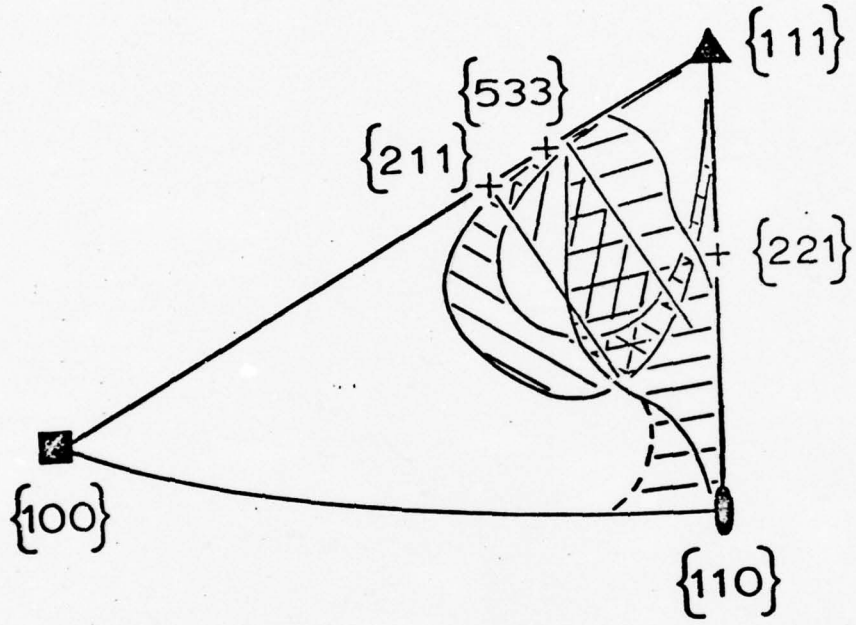

FCC APPARENT
HABIT PLANE

Figure 5

tates of the phenomenological theory, the shear mechanism may still be impossible because the misfit dislocations are in sessile orientation.

3. Experimental Study of the Structure of the Broad Faces of Ferrite Sideplates

This study was made experimentally feasible through use of an Fe-0.63% C-2.05% Si alloy (supplied by the Ford Motor Co.). The high initial carbon content of this alloy ensures that the austenite regions trapped between closely spaced ferrite sideplates will quickly acquire a high and relatively uniform carbon content. Inhibition of cementite precipitation by the high silicon content ensures that the carbon content of the austenite regions is not diminished by this factor. The high carbon content of the trapped austenite regions per se and also the compressive stresses exerted by the ferrite plates on the austenite between them inhibit martensite formation sufficiently well so that even in thin foils regions of retained austenite 0.5 to 1.5 microns thick are present between parallel sideplates in specimens reacted for intermediate times in the temperature range 425°-475°C. These regions are wide enough to permit the tilting and diffraction experiments involved in interfacial structure determinations to be conducted.

The weak-beam, dark-field imaging technique devised by Cockayne (8) has proved suitable for resolving the structure of the broad faces of ferrite sideplates, as illustrated in Figure 6. The α:γ boundary in this Figure has been intercepted at a glancing angle; it is the region containing thick, wriggly, closely spaced thickness contours. The lines running roughly perpendicular to the contours are seen to cause the contours to deflect, and are thus identified as ledges. Arrowheads point out the terminii of one such ledge. Applying the ledge height analysis developed by Gleiter (25) to the contour deflections yields a height of 6-7 Å, or ca. 3 atomic layers, for the ledges. The array of fine, parallel, closely spaced lines in this Figure which does not deflect the thickness contours is composed of misfit dislocations. In this Figure the distance between these dislocations is 18-24 Å.

Also observed at α:γ boundaries, though not shown, are ledges hundreds of Å high

and thousands of Å apart. Ledges of this type were reported by Kinsman, Eichen and Aaronson (26) on ferrite sideplates, as observed primarily by replication electron microscopy; the thickening kinetics of these plates were found to be consistent with the large observed inter-ledge spacings. The ledges shown in Figure 6 are two orders of magnitude more closely spaced and hence (even taking overlap of diffusion fields into account) would lead to thickening rates much higher than those experimentally observed. These considerations support the view that the ledges in Figure 6 are of the structural, rather than of the growth variety.

Interfacial structures similar to Figure 6, and differing only in quantitative details, have been seen at a large number of α:γ boundaries. We are now satisfied that such structures are both representative and generally occurring at these boundaries.

Using the weak-beam, dark-field imaging technique developed by Cockayne (8), seven α:γ boundaries have been studied quantitatively, each under five or more two-beam diffraction conditions, to determine the Burgers vector of the misfit dislocations and of the ledges. Figures 7a-d are typical micrographs of the same area, photographed under different diffraction conditons to determine the Burgers vectors by the $g \cdot b = 0$ method. The misfit dislocations are seen to be out of contrast in Figure 7a, taken with $\underline{g} = [101]_\alpha$, and Figure 7b, taken with $\underline{g} = [020]_\gamma$. For this case, the misfit dislocations were deduced to have a Burgers vector of $\underline{a}/2[\bar{1}01]_\gamma$ or $\underline{a}/2[\bar{1}11]_\alpha$. Table I summarizes all of the results obtained in this manner and compares these results with those obtained from the computer modeling studies. With one partial exception, the values of the spacing, direction, height and Burgers vector of the ledges (ledge heights were determined by the method of Gleiter (25)), the values of the spacing, direction and Burgers vector of the misfit dislocations, and the angle between the structural ledges and the misfit dislocations determined experimentally agree with those predicted by the computer modeling studies. Hence the elaborated-upon structural ledge model of Hall et al (6) and the misfit dislocations added to this model by Russell et al (7) can be considered to have been quantitatively confirmed. F.c.c.:b.c.c. boundaries can now be considered as

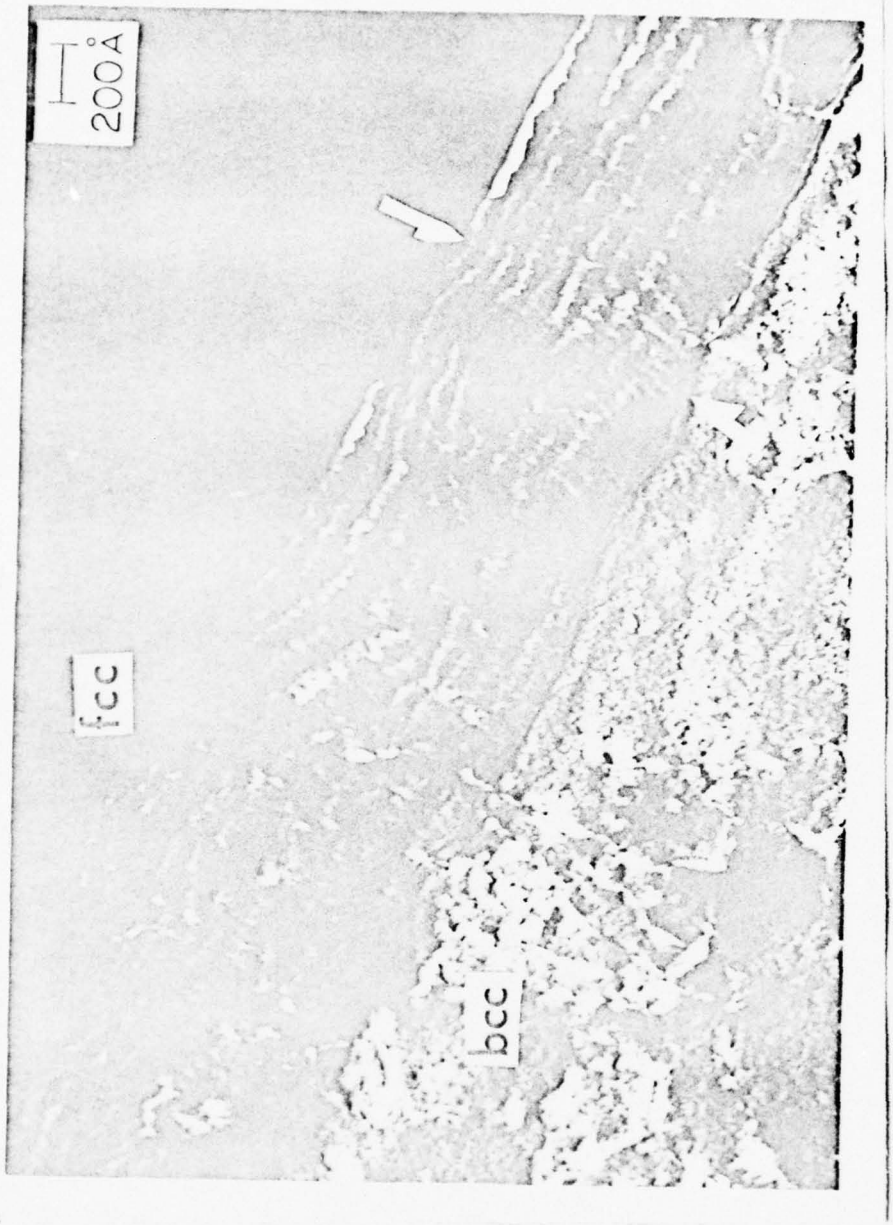

Figure 6

Figure 7(a) 450,000X

Figure 7(b)

Figure 7(c)

Figure 7(d)

Comparison of Observed and Measured Characteristics of Partially Coherent Fcc:Bcc Boundaries on Ferrite Sideplates

AREA	STRUCTURAL LEDGES				DISLOCATIONS			Angle Between Ledge and Dislocation	HABIT PLANE INFORMATION			
	Spacing	Direction	Height	Burgers Vector	Spacing	Direction	Burgers Vector		Apparent FCC Habit Plane	Angle From $(111)_\gamma$	Angle Exp. HP, Model HP	Orientation Relationship*
450°C $A_{(1)}$TEM	37Å	$[\bar{1}01]_\gamma$ 18°ccw	Triat.	incomplete	15Å	$[\bar{1}01]_\gamma$ 48°ccw	incomplete	30°	$(5,8,6)_\gamma$	11°	<2°	1° $01\bar{1}_\gamma$ $00\bar{1}_\alpha$
$A_{(1)}$Model	37.3Å	$[\bar{1}01]_\gamma$ 14°ccw	Triat.	parallel to $[111]_\gamma \| [110]_\alpha$	13Å	$[\bar{1}01]_\gamma$ 50°ccw	a/2 $[\bar{1}10]_\gamma$	36°	$(11,16,12)_\gamma$	9.5°	<2°	same
475°C $A_{(2)}$TEM	22Å	$[\bar{1}01]_\gamma$ 7°cw	Triat.	$[111]_\gamma \| [110]_\alpha$	16.2Å	$[\bar{1}\bar{1}2]_\gamma$ 11°cw	a/2 $[\bar{1}10]_\gamma$ a/2 $[\bar{1}1\bar{1}]_\alpha$	26°	$(15,21,9)_\gamma$	18°	<5°	3° $01\bar{1}_\gamma$ $00\bar{1}_\alpha$
$A_{(2)}$Model	23Å	$[\bar{1}01]_\gamma$ 15°cw	Triat.	$[111]_\gamma \| [110]_\alpha$	16Å	$[\bar{1}\bar{1}2]_\gamma$ 6°ccw	a/2 $[\bar{1}10]_\gamma$ a/2 $[\bar{1}1\bar{1}]_\alpha$	50°	$(5,8,4)_\gamma$	16°	<5°	same
475°C $A_{(3)}$TEM	35Å	$[\bar{1}10]_\gamma$ 4°cw	Triat.	$[111]_\gamma \| [110]_\alpha$	20Å	$[\bar{1}10]_\gamma$ 48°ccw	a/2 $[\bar{1}01]_\gamma$ a/2 $[\bar{1}11]_\alpha$	52°	$(5,5,7)_\gamma$	10°	<2°	3° $01\bar{1}_\gamma$ $00\bar{1}_\alpha$
$A_{(3)}$Model	31.8Å	$[\bar{1}10]_\gamma$ 5°cw	Triat.	$[111]_\gamma \| [110]_\alpha$	20.5Å	$[\bar{1}10]_\gamma$ 44°ccw	a/2 $[\bar{1}01]_\gamma$ a/2 $[\bar{1}11]_\alpha$	49°	$(2,2,3)_\gamma$	11.2°	<2°	2° $01\bar{1}_\gamma$ $00\bar{1}_\alpha$
475°C $A_{(4)}$TEM	44Å	$[11\bar{2}]_\gamma$ 6°cw	Triat.	$[111]_\gamma \| [110]_\alpha$	18Å	$[11\bar{2}]_\gamma$ 19°ccw	a/2 $[\bar{1}10]_\gamma$ a/2 $[\bar{1}1\bar{1}]_\alpha$	25°	$(13,19,15)_\gamma$	9°	<1°	3.5° $00\bar{1}_\alpha$ $01\bar{1}_\gamma$
$A_{(4)}$Model	39.5Å	$[11\bar{2}]_\gamma$ 15°cw	Triat.	$[111]_\gamma \| [110]_\alpha$	16.9Å	$[11\bar{2}]_\gamma$ 4°ccw	a/2 $[\bar{1}10]_\gamma$ a/2 $[\bar{1}1\bar{1}]_\alpha$	19°	$(13,19,15)_\gamma$	9.1°	<1°	3.0° $00\bar{1}_\alpha$ $01\bar{1}_\gamma$
475°C $A_{(5)}$TEM	36Å	$[11\bar{2}]_\gamma$ 13°cw	Triat.	$[111]_\gamma \| [110]_\alpha$	25Å	$[\bar{1}10]_\gamma$ 36°cw	a/2 $[\bar{1}10]_\gamma$ a/2 $[\bar{1}1\bar{1}]_\alpha$	67°	$(9,6,8)_\gamma$	9.3°	<2°	1.5° $00\bar{1}_\alpha$ $01\bar{1}_\gamma$
$A_{(5)}$Model	32.5Å	$[11\bar{2}]_\gamma$ 15°cw	Triat.	$[111]_\gamma \| [110]_\alpha$	27.3Å	$[\bar{1}10]_\gamma$ 32°cw	a/2 $[\bar{1}10]_\gamma$ a/2 $[\bar{1}1\bar{1}]_\alpha$	73°	$(18,11,16)_\gamma$	11°	<2°	1° $00\bar{1}_\alpha$ $01\bar{1}_\gamma$
475°C $A_{(6)}$TEM	36Å	$[11\bar{2}]_\gamma$	Triat.	$[111]_\gamma \| [110]_\alpha$	18Å	$[01\bar{1}]_\gamma$ 10°ccw	a/2 $[\bar{1}10]_\gamma$ a/2 $[\bar{1}1\bar{1}]_\alpha$	40°	$(6,4,5)_\gamma$	9.2°	3°	1.5° $00\bar{1}_\alpha$ $01\bar{1}_\gamma$
$A_{(6)}$Model	32.5Å	$[11\bar{2}]_\gamma$ 15°cw	Triat.	$[111]_\gamma \| [110]_\alpha$	18.3Å	$[01\bar{1}]_\gamma$ 5°cw	a/2 $[\bar{1}10]_\gamma$ a/2 $[\bar{1}1\bar{1}]_\alpha$	40°	$(18,11,16)_\gamma$	11°	3°	1.0° $00\bar{1}_\alpha$ $01\bar{1}_\gamma$
475°C $A_{(7)}$TEM	36Å	$[01\bar{1}]_\gamma$ 13°ccw	Triat.	$[111]_\gamma \| [110]_\alpha$	17Å	$[\bar{1}10]_\gamma$ 22°cw	a/2 $[01\bar{1}]_\gamma$ a $[00\bar{1}]_\alpha$	25°	$(13,19,21)_\gamma$	10.9°	<2°	1° $01\bar{1}_\gamma$ $00\bar{1}_\alpha$
$A_{(7)}$Model	39.5Å	$[01\bar{1}]_\gamma$ 13°ccw	Triat.	$[111]_\gamma \| [110]_\alpha$	16.2Å	$[\bar{1}10]_\gamma$ 16°cw	a/2 $[01\bar{1}]_\gamma$ a $[00\bar{1}]_\alpha$	31°	$(6,8,9)_\gamma$	9.2°	<2°	2.0° $01\bar{1}_\gamma$ $00\bar{1}_\alpha$

Table I

*In all cases, $\{111\}_\gamma \| \{110\}_\alpha$.

classically partially coherent under the appropriate conditions of lattice and boundary orientation with the new feature of structural ledges is incorporated.

Both the experiments and the model show that the misfit dislocations in these boundaries invariably lie in the atomic habit planes, i.e., $\{111\}_\gamma$ and $\{110\}_\alpha$, which constitute the broad faces of the structural ledges. Hence thickening of the ferrite sideplates studied by shear is mechanistically impossible. We hope that this result may contribute significantly to putting an end to the 40+ year old argument as to the mechanism of formation of ferrite and also of bainite plates.

In all cases, the ledges are predicted by the model and found experimentally to be triatomic. The prediction was based upon minimization of interfacial energy. This outcome is of particular interest because triatomic structural ledges have the unique property of allowing the apparent f.c.c.:b.c.c. interface to deviate from $\{111\}_\gamma$ in either a clockwise or a counterclockwise direction br stepping "up" or "down". It would appear that this property of triatomic ledges may explain an important part of the often observed tendency of ferrite plates to exhibit waviness when viewed at high magnifications.

The wide variety of the apparent habit planes found and their usually quite irrational character makes clear that no direct structural significance should be attached to such planes when present in a diffusional transformation. It should also be clear that irrational habit planes are no longer to be considered a unique property of martensitic transformations.

B. Stereology and Growth Kinetics of Grain Boundary Ferrite Allotriomorphs in Fe-C Alloys

1. Introduction

Although an appreciable amount of data are already available on the growth kinetics of grain boundary allotriomorphs of proeutectoid ferrite in Fe-C alloys (26-28), not all of it is on lengthening as well as thickening kinetics, the data encompasses an insufficiently large envelope of carbon content and reaction temperature to serve as "baseline" information for all of the Fe-C-X studies projected on this Grant and the scatter in much of this data is sufficiently large so that comparison of growth kinetics data in different alloys is significantly hampered.

Most of the previous data on allotriomorph growth kinetics were obtained by means of thermionic emission microscopy. Since such an instrument is not available at Michigan Technological University, a room temperature technique previously employed (17) was further developed which permitted the necessary measurements to be made with available equipment. This method consists of preparing specimens which are sufficiently thin and austenitizing them for a combination of temperature and time adequate to ensure that nearly all of the austenite grain boundaries become perpendicular to the broad faces of the rectangular parallelpiped-shaped specimens. The specimens are reacted for a series of successively increasing times at each temperature. In each specimen, the length of the longest and the thickness of the thickest grain boundary allotriomorph is measured. Allotriomorphs which are malformed as a result of faceting are excluded from measurement of either dimension. The slope of plots of the half-length and half-thickness vs. the square root of the isothermal reaction time (properly, of the growth time, but the difference in Fe-C alloys is neither large nor consistent) yields the parabolic rate constants β and α for lengthening and thickening, respectively.

Although the thermionic emission microscopy method of measuring growth kinetics is highly precise, concentrating as it does on individual allotriomorphs while they are actually growing at the temperature of transformation, the different proportion and disposition of facets on allotriomorphs formed at different grain boundaries has been previously recognized (26) as contributing substantially to the scatter in the plots of parabolic rate constant vs. reaction temperature through which these data are reported. It was therefore considered that the method employed in the present investigation would reduce this scatter by emphasizing the largest, and thus the least facet-hampered allotriomorphs. This procedure was expected to more than compensate for the errors inevitably introduced when each data point represents a separately heat-treated specimen. This expectation appears to have been fulfilled. However, a portion of the superiority of the present room temperature method evidently derives from its inherent stereological advantages over any hot stage method. The results of the stereological analysis upon which this conclusion is based are summarized in the next subsection; in

the following subsection, the results of the experimental measurements are reported.

2. Stereology of Grain Boundary Allotriomorphs

DeHoff (29) has published an elegant stereological analysis of both the nucleation and the growth of precipitates which are assumed to have an idealized form. For the purposes of the present investigation, however, it was decided to devise a new, more specialized analysis, dealing only with the growth process. The primary reasons for this decision are that DeHoff's assumption of an idealized shape is not too often met by ferrite allotriomorphs and that the grain boundary geometry intentionally established results in specialized, rather than random sectioning of the allotriomorphs.

The heavily outlined area of Figure 8a is a polar cross-section through the idealized grain boundary allotriomorph upon which the calculations of this study are based. When the allotriomorph is sectioned perpendicular to the grain boundary a distance X_o from its center, the section of the allotriomorph shown in Figure 8b appears on the plane of polish. The true length, L, and true thickness, S, of the allotriomorph are now replaced by apparent, and different values, L' and S' respectively. The true dihedral angle, ϕ, at the edges of the allotriomorph is now replaced by an apparent one, ϕ_{app}. The apparent shape of the allotriomorph, however, remains symmetrical. When the allotriomorph is sectioned by a plane of polish which lies both X_o from the allotriomorph center and also forms an angle ψ with respect to a normal to the grain boundary plane, as in Figure 9a, the allotriomorph now appears asymmetrical on the plane of polish, with two different apparent thicknesses, S_1 and S_2, and two different "half" dihedral angles, ϕ_1 and ϕ_2, as illustrated in Figure 9b. However, the apparent length of the allotriomorph is a function only of X_o, not of ψ.

Equations were derived connecting true and apparent values of length, thickness, aspect ratio and dihedral angle as a function of both X_o and ψ. These relationships were then used, in conjunction with the Horvay-Cahn (30) relationships for the thickening and lengthening of an oblate ellipsoid ($S/2 = \alpha t^{1/2}$ and $L/2 = \beta t^{1/2}$, where α and β are the respective parabolic growth rate constants and t = growth time), to derive

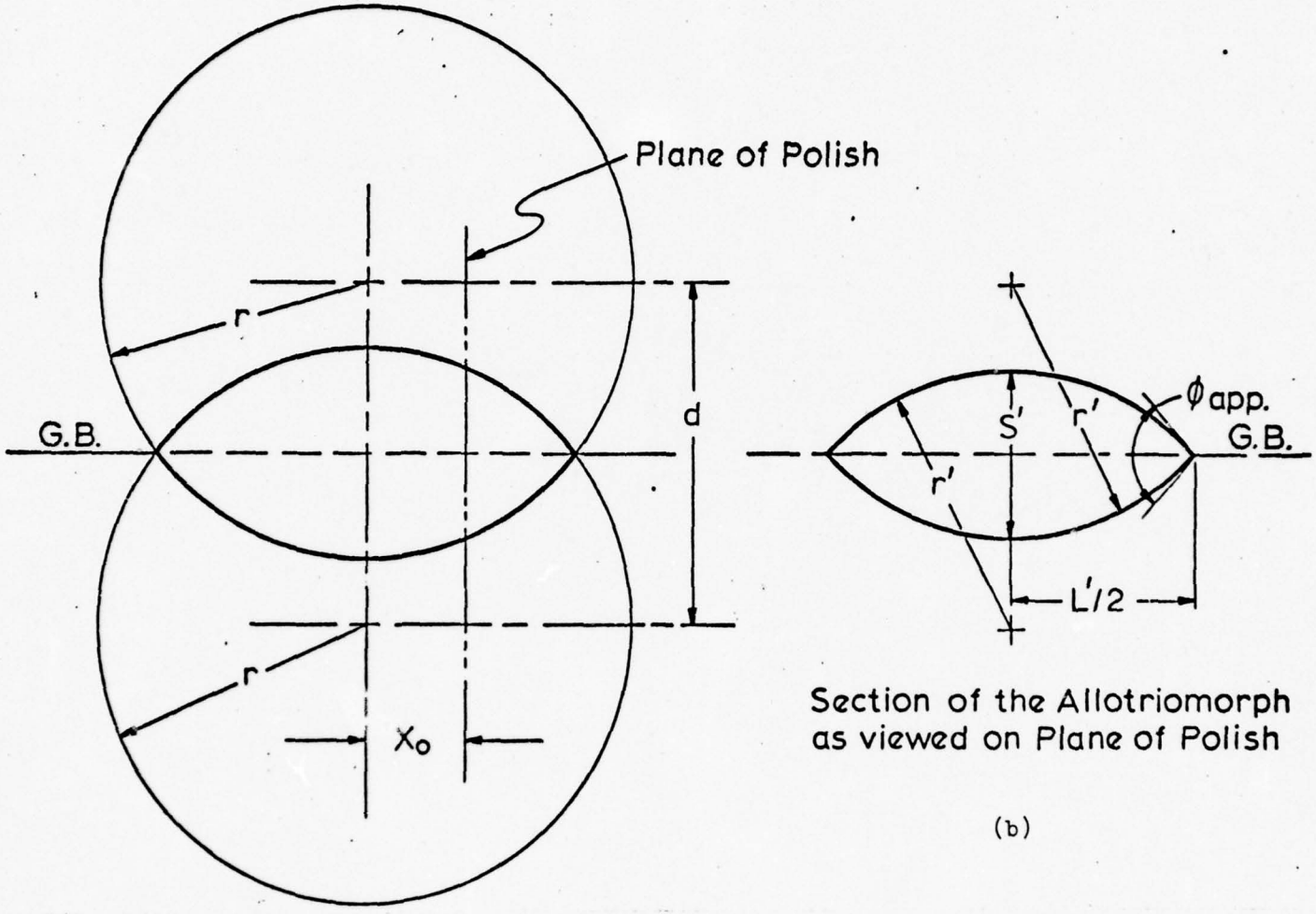
Plane of Polish
r
G.B.
d
r
X_o
(a)
ϕ app.
S'
r'
G.B.
r'
L'/2
Section of the Allotriomorph
as viewed on Plane of Polish
(b)

Figure 8

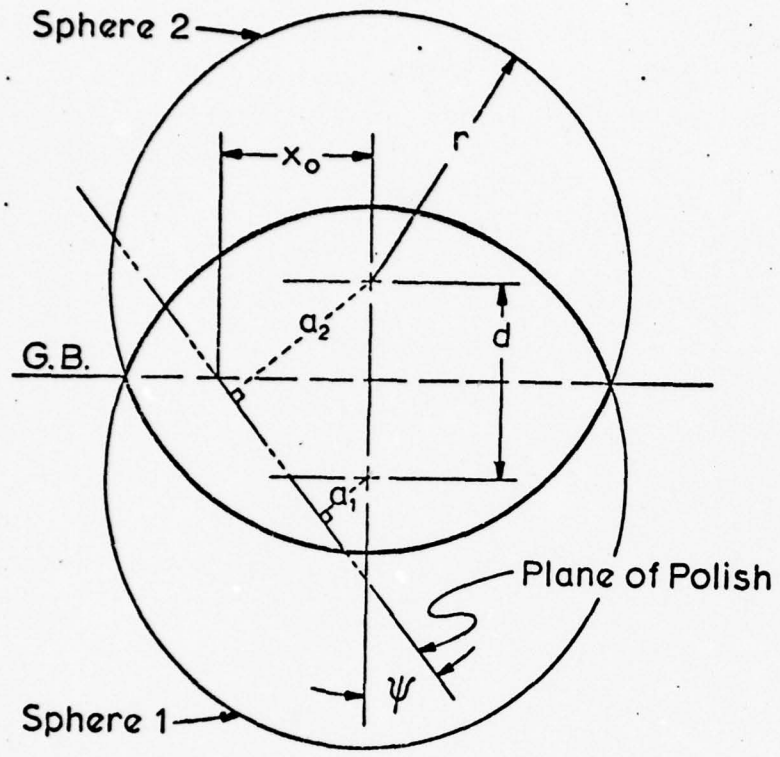

(a)

Section of the Allotriomorph as viewed on Plane of Polish

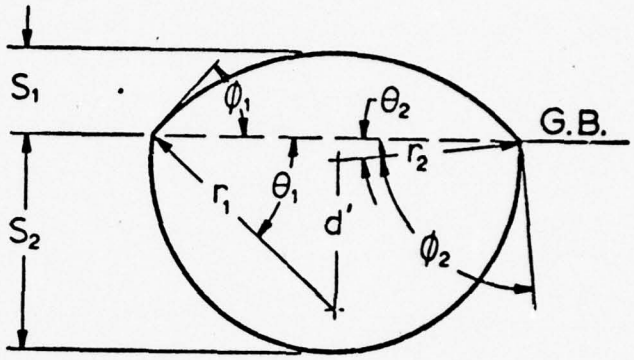

(b)

Figure 9

equations for the apparent parabolic rate constants as functions of X_o, ψ and true growth rates. It was shown that only when an allotriomorph is sectioned so that $X_o = \psi = 0$ will the apparent parabolic rate constants be actually independent of reaction time, and correct. When $X_o \neq 0$ and $\psi = 0$, the apparent aspect ratio (α_{app}/β_{app}) and the apparent dihedral angle will increase during growth and approach their true values. When $X_o = 0$ and $\psi \neq 0$, both the apparent aspect ratio and the apparent dihedral angle will be constant; both, however, will be greater than their true values. When $X_o \neq 0$ and $\psi \neq 0$, both apparent aspect ratio and apparent dihedral angle will vary with time and attain values greater than their true ones.

The apparent growth rate equations thus obtained were combined with the growth rates experimentally measured by the room temperature sectioning technique for an Fe-0.11% C alloy (as reported in the next subsection) to estimate the proportion of the scatter in thermionic emission microscopy growth rate data previously reported (27) on the same alloy which might be attributed to stereological factors. The apparent half-thickness of allotriomorphs nucleated from 0 to 100 microns beneath the plane of polish was calculated as a function of the apparent growth time for $\psi = 0°$, 30° and 45°, using the experimental values obtained during the present study for the true rate constants at each of several reaction temperatures. Apparent growth rate constants are then obtained as the slope of a least squares line fitted to plots of apparent half-thickness and apparent half-length vs. (apparent growth time)$^{1/2}$ under various conditions of X_o and ψ. Figures 10 and 11 show the ratio $\alpha_{app}/\alpha_{true}$ as a function of X_o for all three values of ψ at the highest and lowest reaction temperatures studied in the 0.11% C alloy.

Clearly, a wide range of apparent rate constants is possible, $\alpha_{app}/\alpha_{true}$ varying from ca. 1.9 to ca. 0.1 at $\psi = 45°$. Even at $\psi = 0°$ a substantial error is possible due to the effect of sectioning away from the center of the allotriomorph, though in this case the apparent parabolic rate constants are limited almost entirely to values which are too small. The upper and lower limits of the range of possible stereological scat-

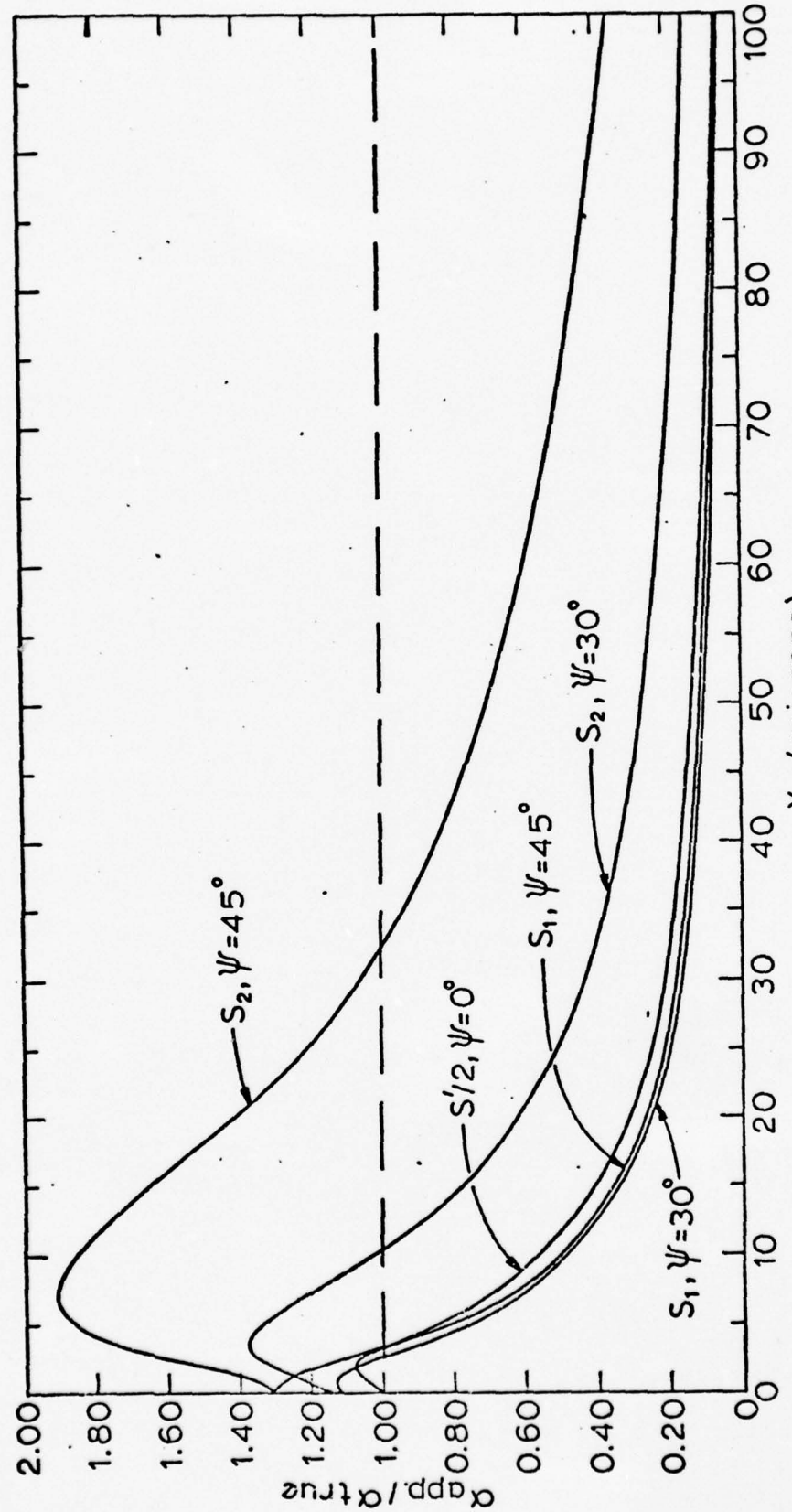
2.00
1.80
1.60
1.40
1.20
1.00
0.80
0.60
0.40
0.20
0
$\alpha_{app}/\alpha_{true}$
0
10
20
30
40
50
60
70
80
90
100
X_o (microns)
$S_2, \psi=45°$
$S'/2, \psi=0°$
$S_1, \psi=45°$
$S_2, \psi=30°$
$S_1, \psi=30°$

Figure 10

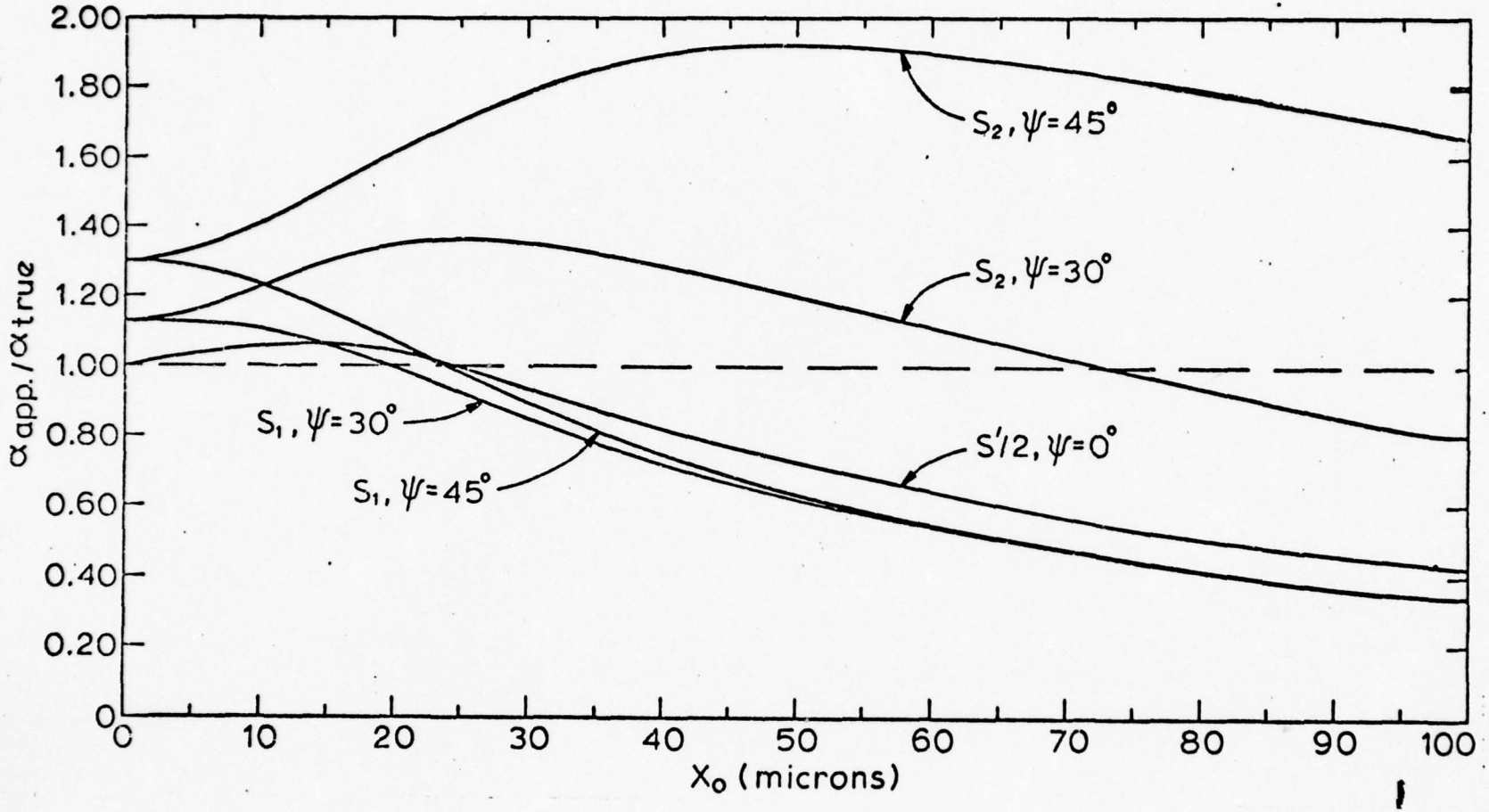
2.00
1.80
1.60
1.40
1.20
1.00
0.80
0.60
0.40
0.20
0
0
10
20
30
40
50
60
70
80
90
100
$\alpha_{app.}/\alpha_{true}$
X_o (microns)
$S_2, \psi=45°$
$S_2, \psi=30°$
$S_1, \psi=30°$
$S_1, \psi=45°$
$S'/2, \psi=0°$

Figure 11

ter for each value of ψ was determined by passing a line through the maximum and minimum values of α_{app} as a function of temperature, taken from the plots of $\alpha_{app}/\alpha_{true}$ vs. X_o. The resulting scatter bands are plotted in Figure 12, together with the data on α in an Fe-0.11% C alloy obtained by thermionic emission microscopy (26,27). It can be seen that approximately one-quarter or one-half of the thermionic emission data falls within the stereological scatter band, depending upon whether ψ is assumed to be 30° or 45°.

In the light of the foregoing considerations, the relative merits of the room temperature sectioning and hot stage methods of measuring the growth kinetics of grain boundary allotriomorphs may be evaluated. Hot stage measurement techniques, such as thermionic emission, provide highly precise data on the apparent growth kinetics of individual allotriomorphs. However, significant errors may result under conditions when X_o and $\psi \neq 0$. The room temperature technique, on the other hand, causes both X_o and ψ to approach zero -- quite closely if a sufficient number of allotriomorphs is measured. Hence even though the parabolic rate constants determined by the room temperature technique are less precise than those obtained from a hot stage method, they are more accurate. Although errors due to ψ can be minimized when specimens are solution annealed so as to make as many of the grain boundaries essentially perpendicular to the intended plane of polish, those caused by $X_o \neq 0$ cannot be similarly controlled. Hence the room temperature technique turns out, somewhat unexpectedly, to yield more accurate values of the parabolic rate constants.

A stereological analysis was also made of the dihedral angles expected at the edges of allotriomorphs when X_o and $\psi \neq 0$. Although the frequency histograms of the various apparent dihedral angles are now differently shaped than those calculated by C. S. Smith (33), the basic conclusion of Smith's analysis, namely that the angle occurring most frequently on the histogram is the true angle, is retained under the more specialized conditions of sectioning assumed in this analysis.

3. Growth Kinetics of Grain Boundary Ferrite Allotriomorphs

The objectives of this investigation were to test the room temperature

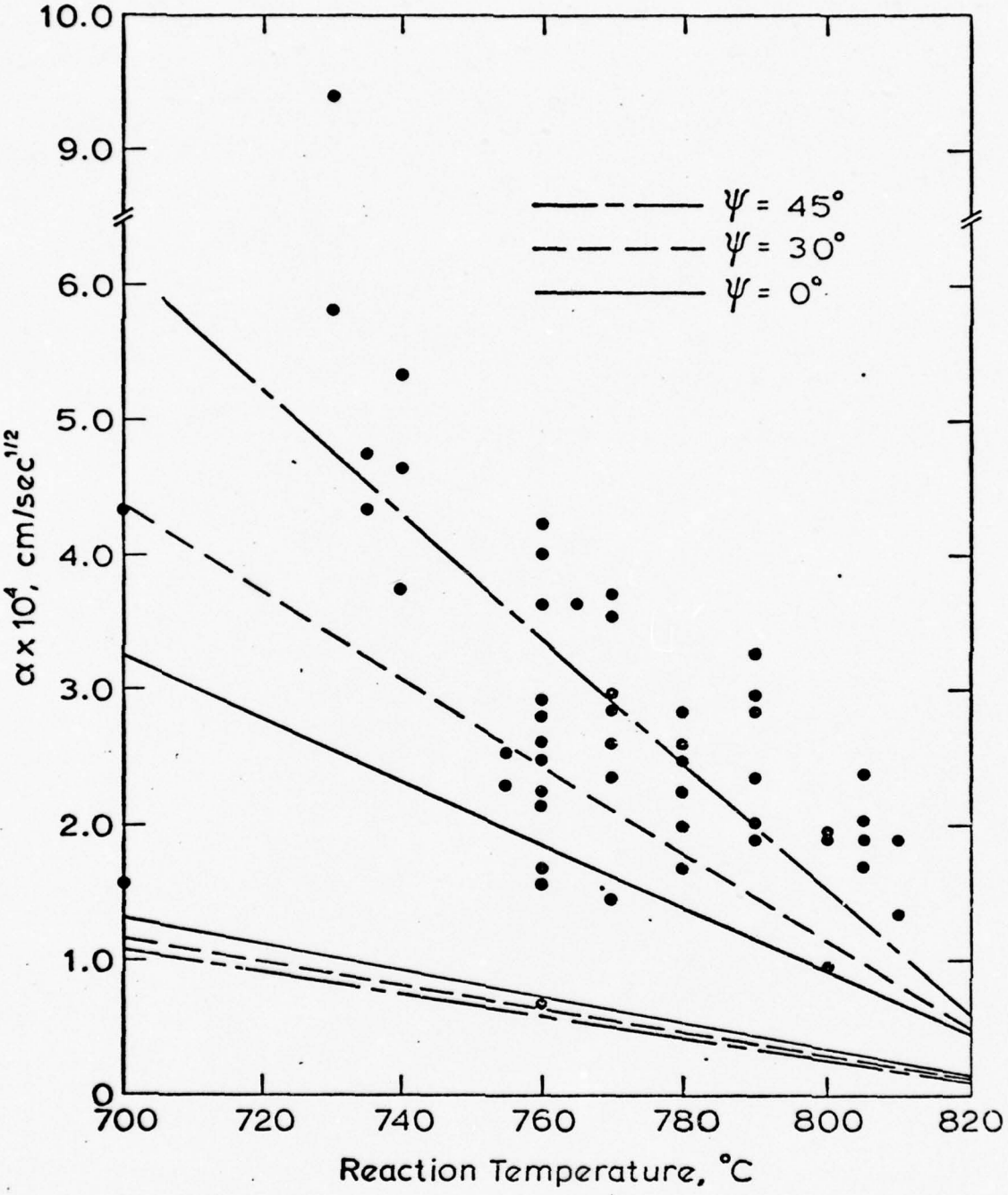
10.0
9.0
6.0
5.0
4.0
3.0
2.0
1.0
0
ψ = 45°
ψ = 30°
ψ = 0°
α x 10⁴, cm/sec¹/²
700
720
740
760
780
800
820
Reaction Temperature, °C

Figure 12

technique of measuring the lengthening and thickening kinetics of grain boundary ferrite allotriomorphs, to document these kinetics over the range of carbon contents and reaction temperatures of interest in the follow-on studies of allotriomorph growth kinetics in Fe-C-X alloys and to take advantage of the reduced scatter anticipated in these data to ascertain the validity of the deviations from carbon diffusion-controlled growth kinetics observed during previous thermionic emission microscopy studies of allotriomorph growth kinetics in Fe-C alloys (26-28). A subsidiary objective was to expand sufficiently the envelope of temperature and carbon content in which data on these kinetics are available to ensure that conclusions drawn from such information have an adequately broad experimental base.

Three high-purity Fe-C alloys, containing 0.11, 0.23 and 0.42 W/O C, were employed. Individual specimens, 0.64 x 0.64 x 0.025 cm., were austenitized for 15 min. at 1300°C in a graphite-deoxidized, argon-protected bath of molten $BaCl_2$, isothermally reacted in graphite-deoxidized lead baths and then quenched into iced 10% brine. As previously indicated, the length of the longest and the thickness of the widest grain boundary allotriomorph was determined in specimens reacted for successively increasing times at each temperature investigated. Measurements were not made on badly faceted allotriomorphs or any grain boundary-nucleated precipitates not strictly allotriomorphic in shape. Measurements were also made of the dihedral angle at the tips of allotriomorphs in representative specimens. Transmission and scanning electron studies were made of the broad faces of allotriomorphs to ascertain whether or not fine-scale faceting is present.

Typical plots of half-length and half-thickness vs. $(\text{reaction time})^{1/2}$ are shown in Figure 13, together with the least squares parabolic rate constant calculated for each plot, and the aspect ratio for the reaction temperature -- taken as α/β. In order to be certain that the data used in constructing such plots are valid, all of it was also replotted as ln (half-thickness) or ln (half-length) vs. ln (growth time), as shown in Figure 14 for the data Figure 13. According to Horvay-Cahn (30) theory, the slope

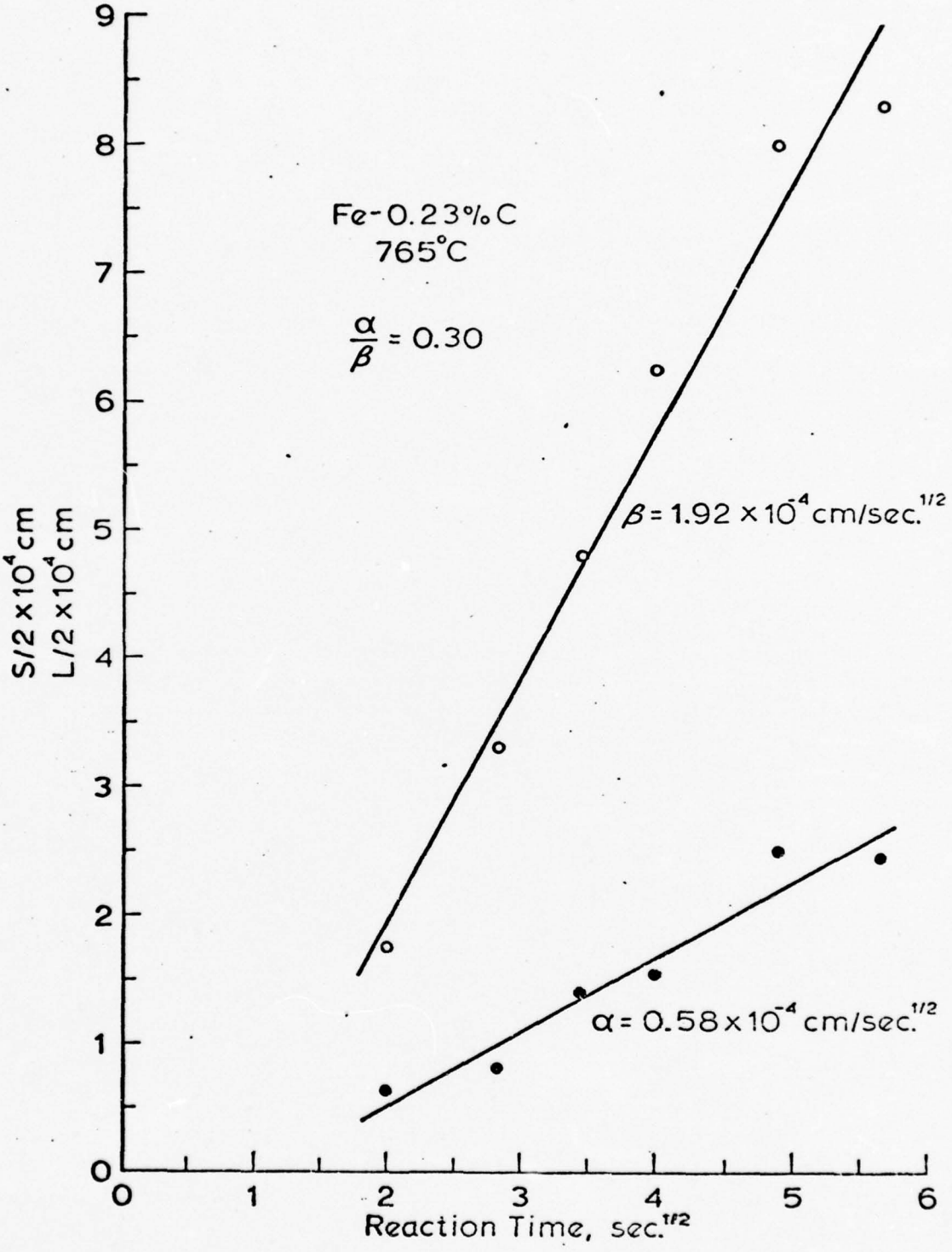
Fe-0.23% C
765°C
α/β = 0.30
β = 1.92 × 10⁻⁴ cm/sec.^1/2
α = 0.58 × 10⁻⁴ cm/sec.^1/2
S/2 × 10⁴ cm
L/2 × 10⁴ cm
Reaction Time, sec.^1/2
0
1
2
3
4
5
6
7
8
9

Figure 13

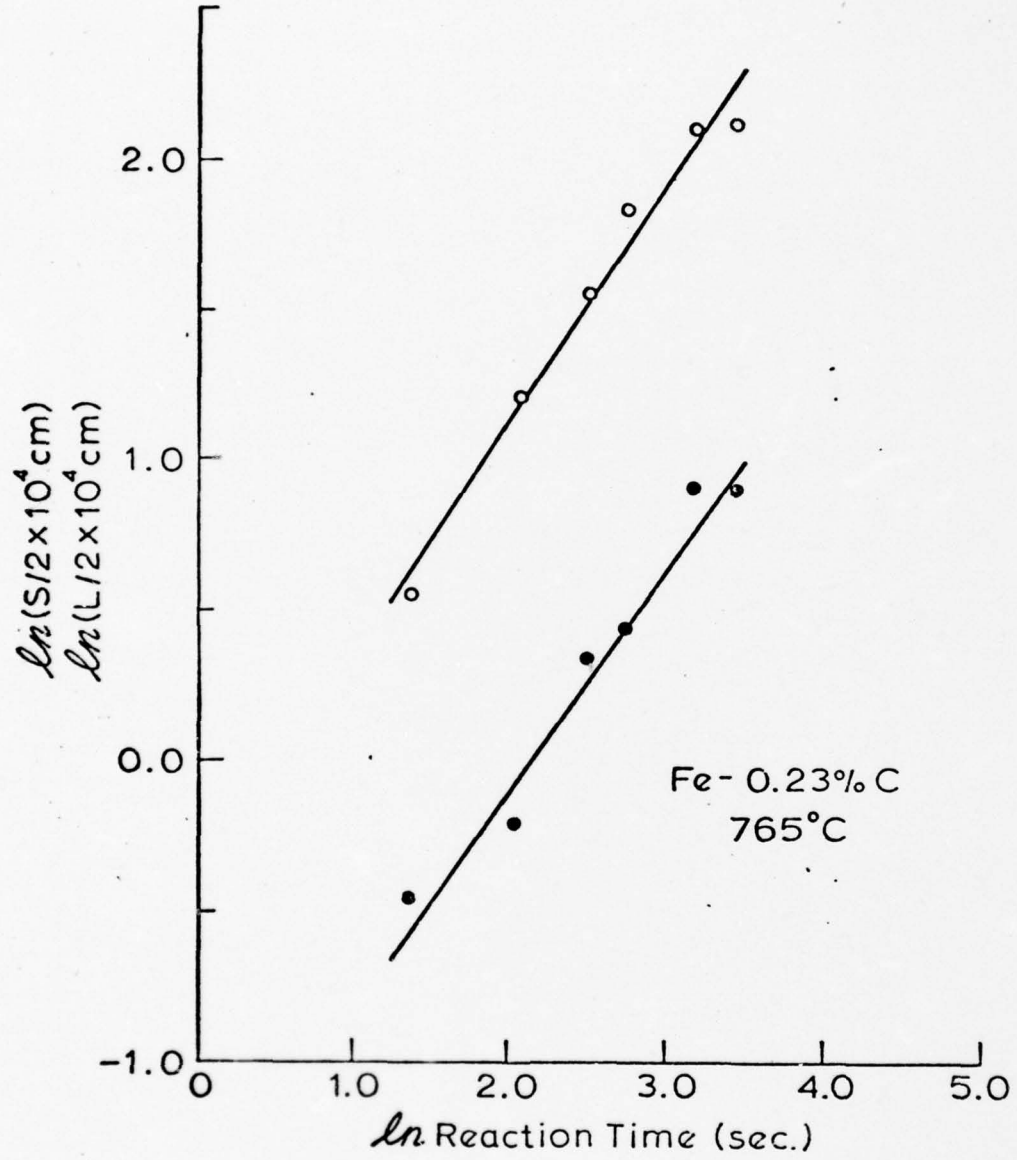
2.0
1.0
0.0
-1.0
0
1.0
2.0
3.0
4.0
5.0
ln (S/2 x 10⁴ cm)
ln (L/2 x 10⁴ cm)
ln Reaction Time (sec.)
Fe - 0.23% C
765°C

Figure 14

of such plots should be 1/2. Figure 15 shows, again typically, that this stricture is fulfilled by the data used. However, at the lowest reaction temperature initially used for all three alloys, values of the slope significantly greater than 1/2 were obtained. These are presumably the results of transformation during quenching to the reaction temperature; such data were not further considered. Figures 16-18 show the measured parabolic rate constants for thickening and lengthening as a function of reaction temperature for all three alloys. Both α and β are seen to decrease with temperature in a regular manner. When these data for the 0.11% C alloy were compared with the thermionic emission data (26,27) obtained on the same alloy and only those thermionic emission data were included for which the aspect ratio was ca. 1/3 (the average found for allotriomorphs during this investigation -- see below), then reasonable agreement was obtained between the two sets of data and the scatter in each was comparable (Figure 19). However, when all of the thermionic emission data were included in the comparison, the scatter of the present data was much less, thereby fulfilling the expectation for the stereological superiority of the room temperature technique. Also included in Figures 16-18 are plots of α and β vs. temperature, calculated via computer from Atkinson's (27,31) analysis for the growth kinetics of an oblate ellipsoid under the assumption that the aspect ratio, $K = 1/3$. The experimental rate constants are seen to be less than those calculated at each reaction temperature used in all three alloys. This result is better demonstrated by the (typical) plots of α(experimental)/α(calculated) and of β(experimental/β(calculated) vs. temperature shown in Figure 20 for the 0.11% C alloy. These ratios are seen to increase systematically from ca. 0.1 at the highest temperature studied to ca. 0.7-0.8 at the lowest temperature.

Previous investigators (26) have proposed that behavior of this type -- now considerably more securely documented -- is due to faceting on the broad faces of the allotriomorphs. With decreasing temperature, growth of disordered portions of the α:γ boundaries round the facets becomes easier as a result of the more rapid growth kinetics at these temperatures. The scanning electron micrograph of Figure 21, and also

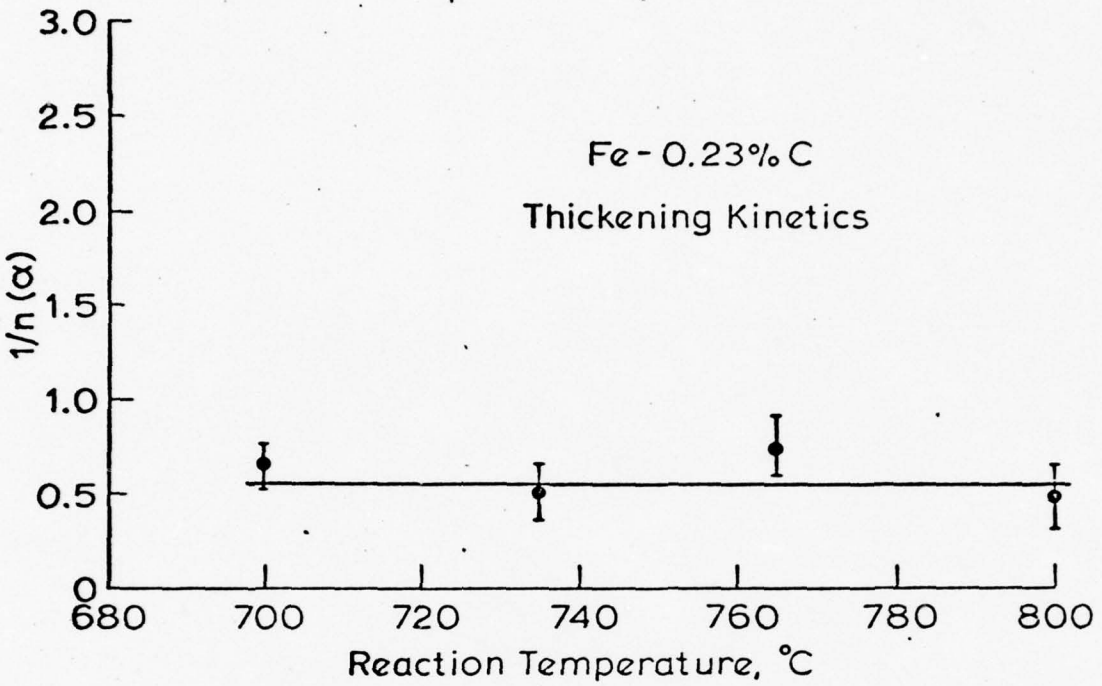
3.0
2.5
2.0
1.5
1.0
0.5
0
1/n (α)
Fe - 0.23% C
Thickening Kinetics
680
700
720
740
760
780
800
Reaction Temperature, °C

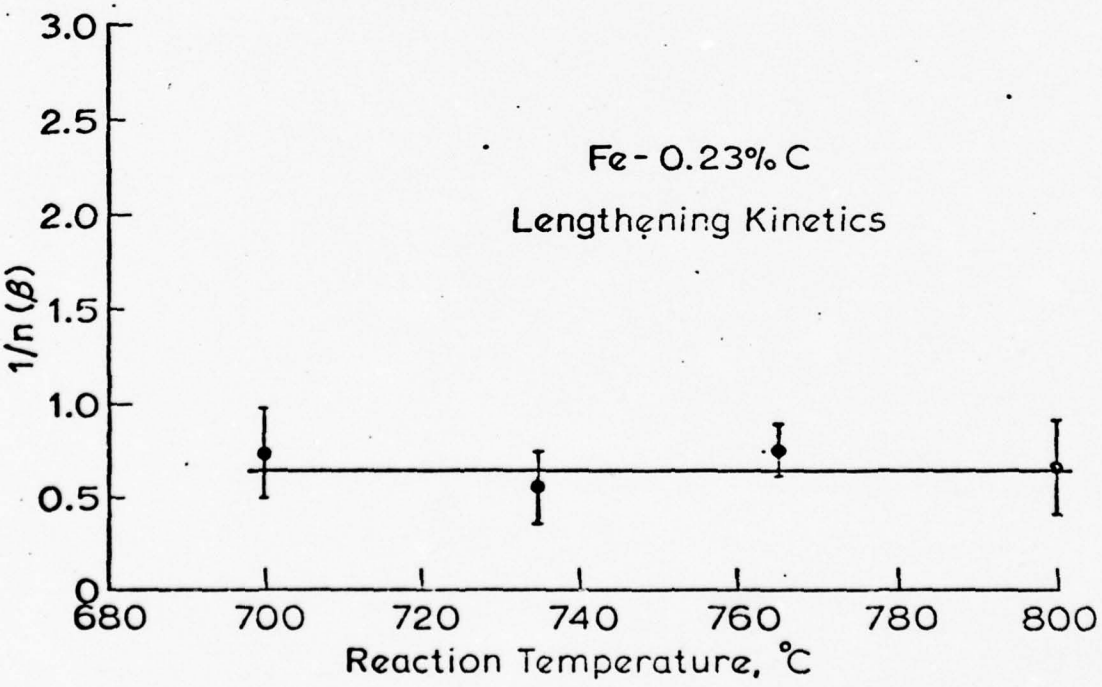
3.0
2.5
2.0
1.5
1.0
0.5
0
1/n (β)
Fe - 0.23% C
Lengthening Kinetics
680
700
720
740
760
780
800
Reaction Temperature, °C

Figure 15

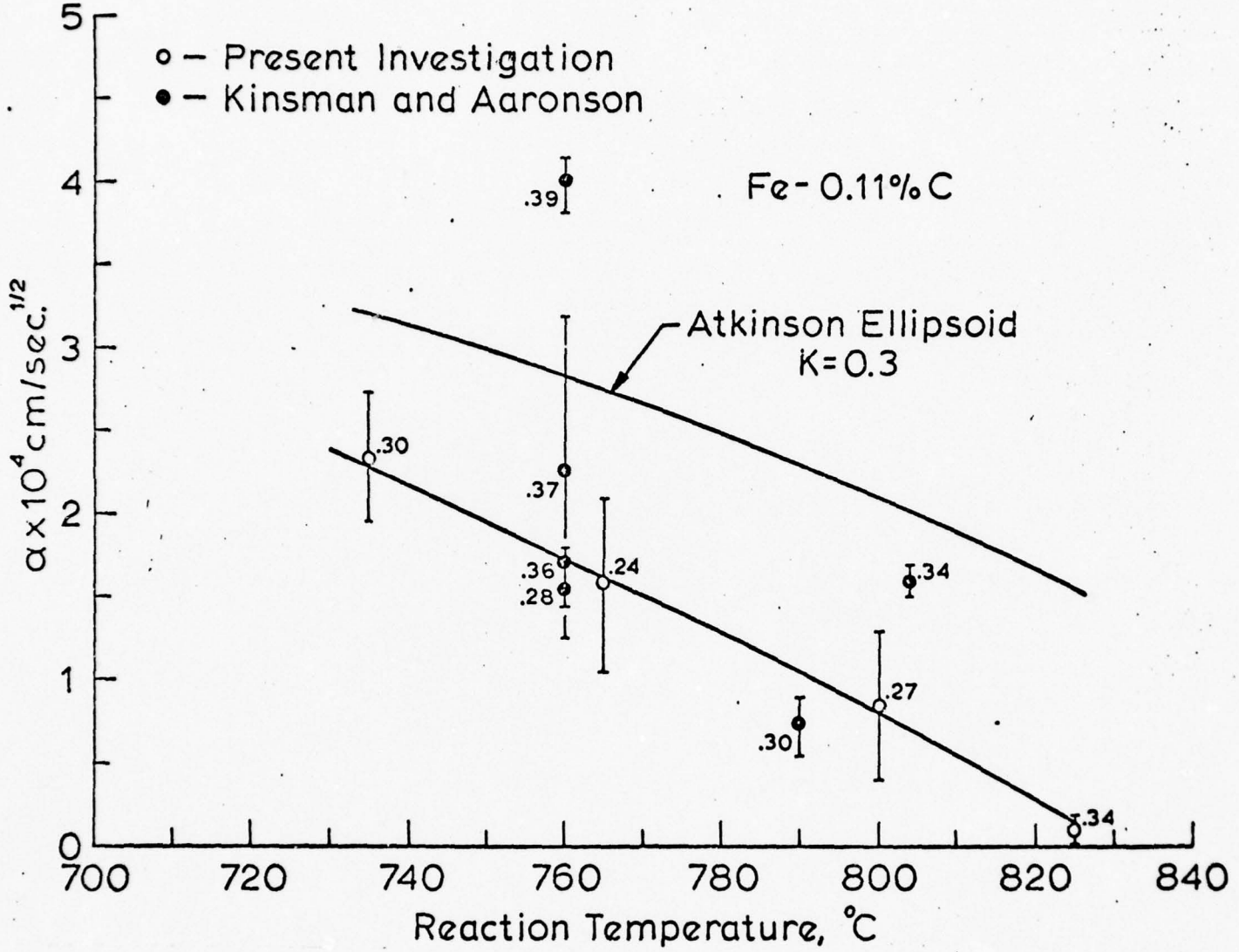
o — Present Investigation
• — Kinsman and Aaronson
Fe - 0.11% C
Atkinson Ellipsoid
K = 0.3
$\alpha \times 10^4$ cm/sec.$^{1/2}$
Reaction Temperature, °C
0
1
2
3
4
5
700
720
740
760
780
800
820
840
.39
.30
.37
.36
.28
.24
.34
.30
.27
.34

Figure 16a

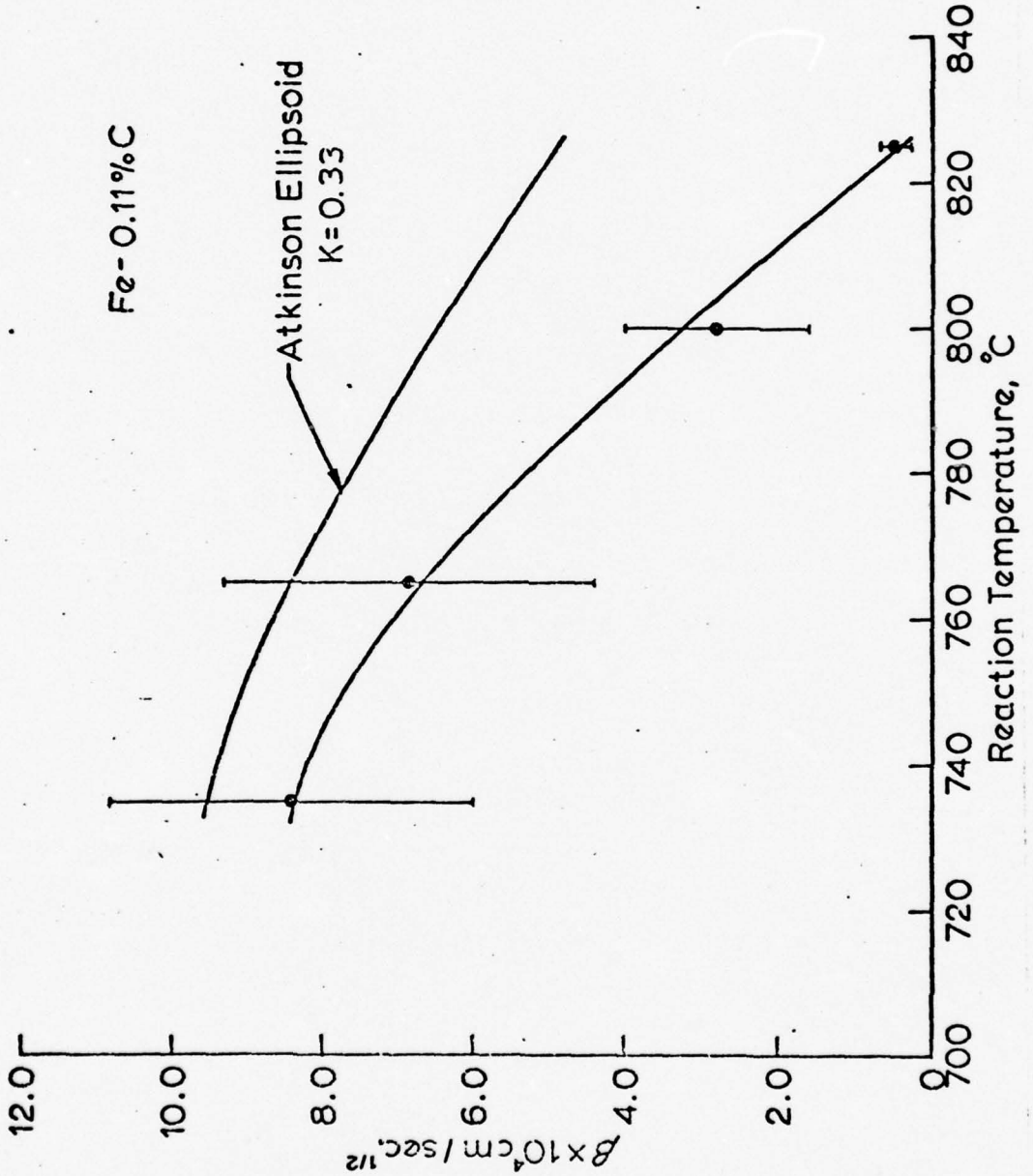
Fe-0.11%C
Atkinson Ellipsoid
K=0.33
12.0
10.0
8.0
6.0
4.0
2.0
0
700
720
740
760
780
800
820
840
Reaction Temperature, °C
β x 10⁴ cm / sec.^1/2

Figure 16b

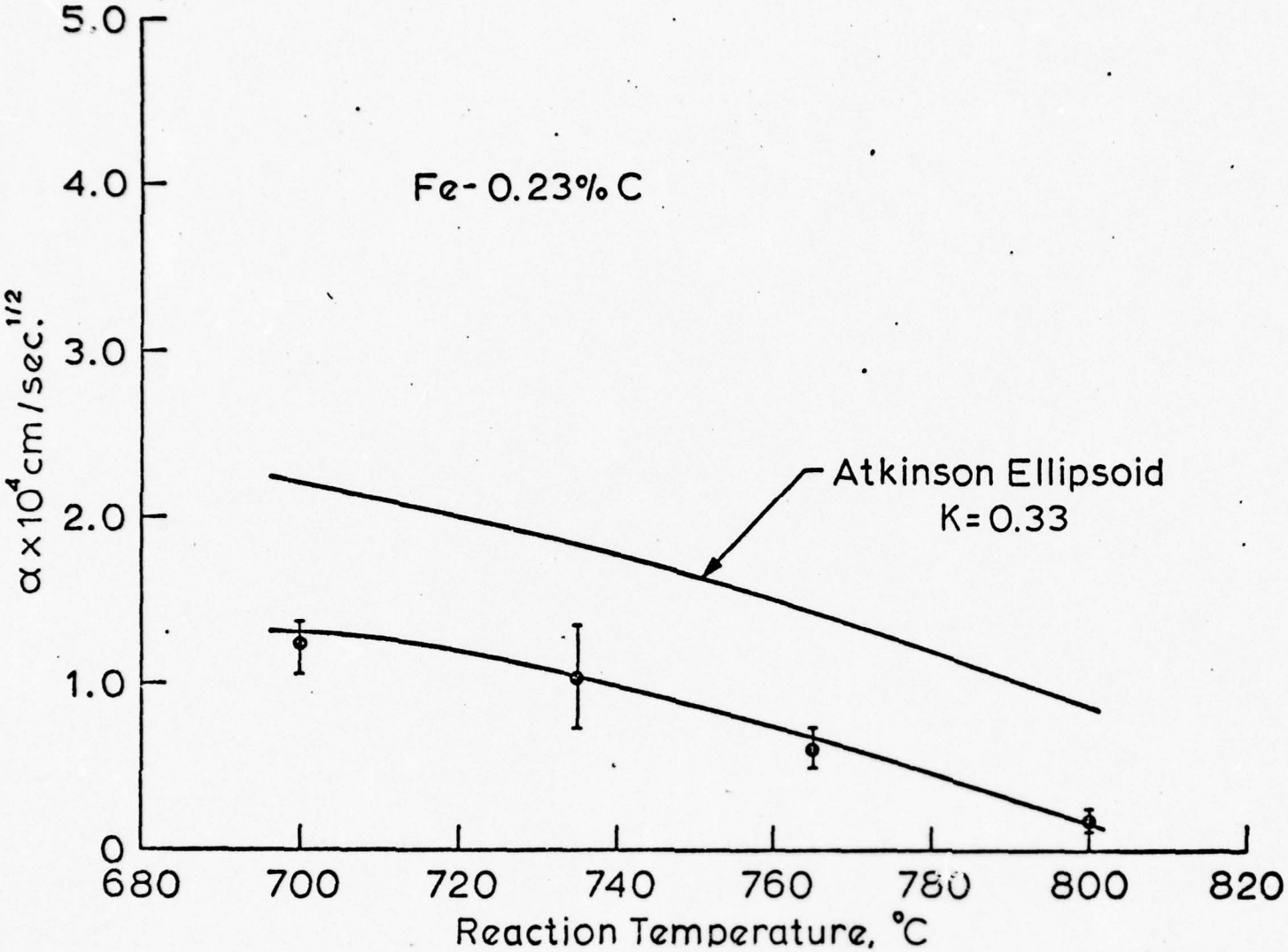
5.0
4.0
3.0
2.0
1.0
0
Fe- 0.23% C
Atkinson Ellipsoid
K= 0.33
α x 10^4 cm / sec.^1/2
680
700
720
740
760
780
800
820
Reaction Temperature, °C

Figure 17a

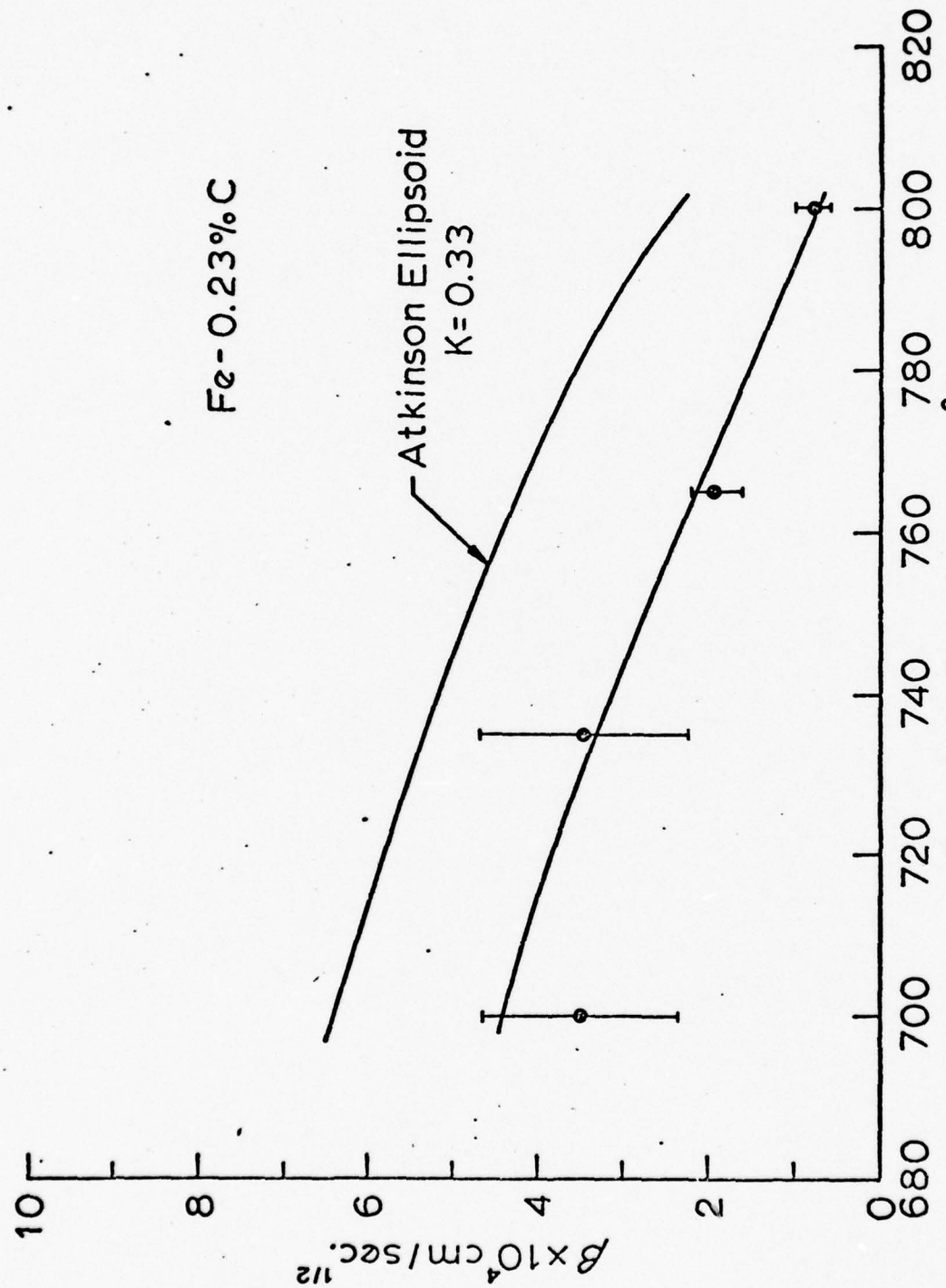
Fe-0.23%C
Atkinson Ellipsoid
K=0.33
$\beta \times 10^4$ cm/sec.$^{1/2}$
Reaction Temperature, °C
0
2
4
6
8
10
680
700
720
740
760
780
800
820

Figure 17b

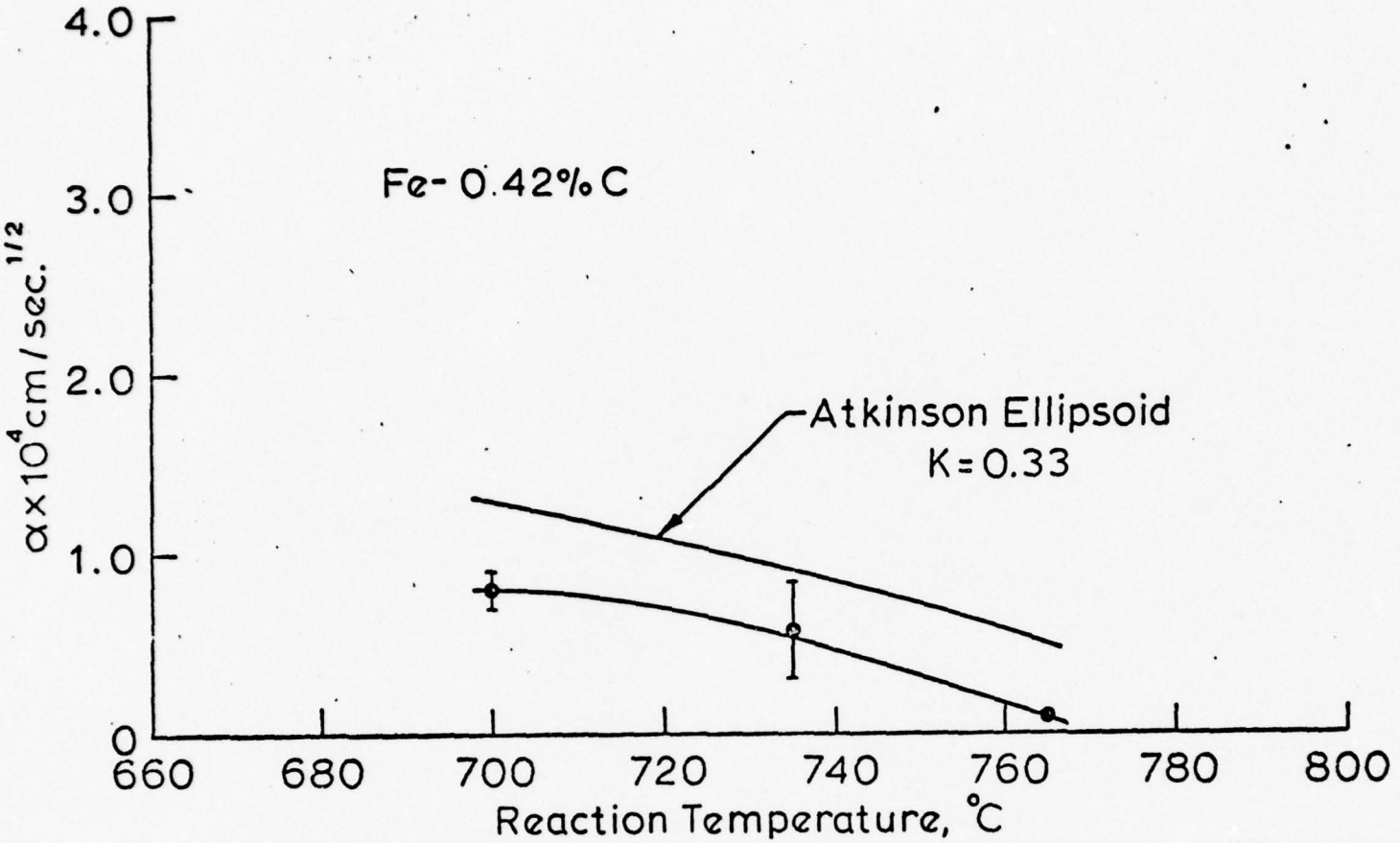
Fe- 0.42% C
Atkinson Ellipsoid
K = 0.33
$\alpha \times 10^4$ cm / sec.$^{1/2}$
4.0
3.0
2.0
1.0
0
660
680
700
720
740
760
780
800
Reaction Temperature, °C

Figure 18a

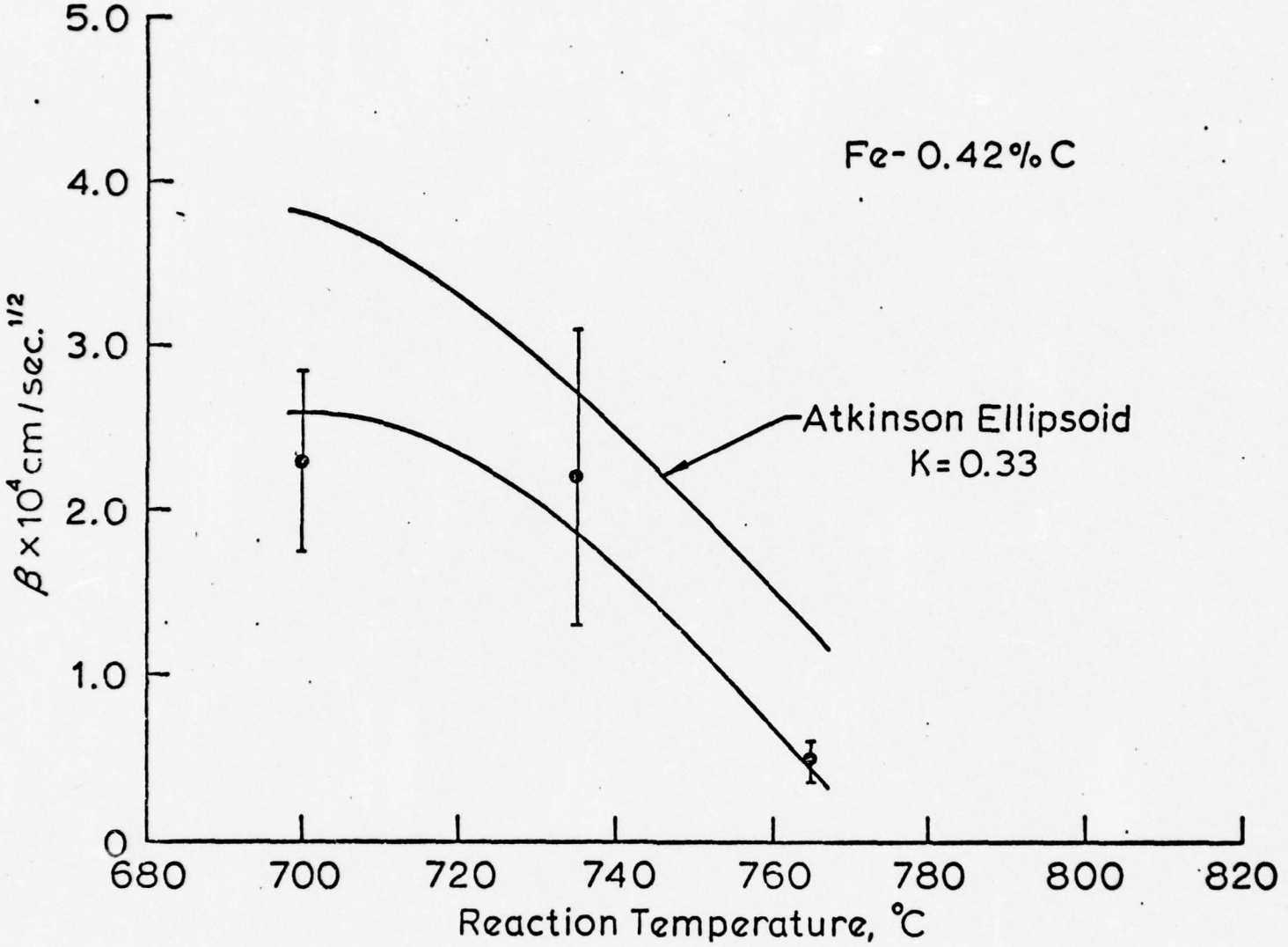
5.0
4.0
3.0
2.0
1.0
0
$\beta \times 10^4$ cm/sec.$^{1/2}$
Fe- 0.42% C
Atkinson Ellipsoid
K= 0.33
680
700
720
740
760
780
800
820
Reaction Temperature, °C

Figure 18b

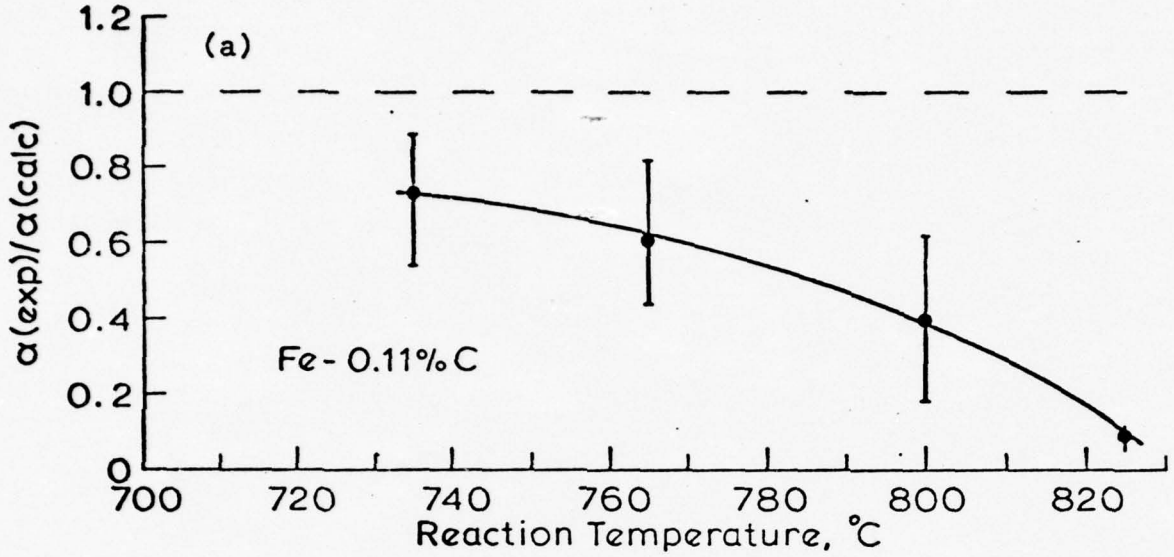
(a)
α(exp)/α(calc)
1.2
1.0
0.8
0.6
0.4
0.2
0
Fe - 0.11% C
700
720
740
760
780
800
820
Reaction Temperature, °C

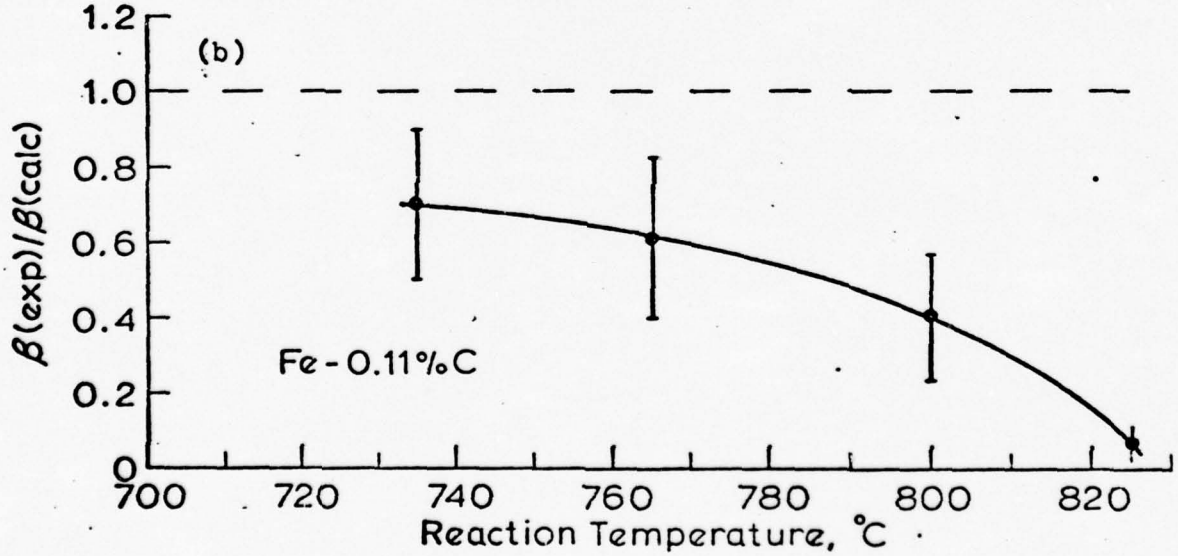
(b)
β(exp)/β(calc)
1.2
1.0
0.8
0.6
0.4
0.2
0
Fe - 0.11% C
700
720
740
760
780
800
820
Reaction Temperature, °C

Figure 20

0.6μ

Figure 21

transmission electron micrographs, support this view by displaying facets on a typical allotriomorph. The proposal of D. E. Coates (32) that measured rate constants for ferrite allotriomorphs which fall no further below those calculated from the Atkinson analysis in Fe-C-X alloys than the ratios of Figure 20 are the result of alloying element partition between austenite and ferrite at higher reaction temperatures is thus shown to be without experimental support. Not unless the planned measurements on allotriomorph growth kinetics in Fe-C-X alloys show significantly smaller ratios of the experimental to the calculated parabolic rate constants can such kinetic data be taken as evidence that another effect, such as that arising from alloying element partition, is superimposed the effect of faceting. Hence the importance of the kinetic data on Fe-C alloys for the planned studies on Fe-C-X alloys is clearly illustrated.

A new result obtained from the present study is that the aspect ratio of ferrite allotriomorphs in Fe-C alloys is ca. 1/3, independent of isothermal reaction time (Figure 22), reaction temperature (Figure 23) and carbon content (Figure 24).

In an effort to understand this rather striking result on an interfacial energy basis, apparent dihedral angles at the tips of ferrite allotriomorphs were measured in the 0.11% C alloy at 735°C and in the 0.42% C alloy at 735° and 765°C, in each case at four reaction times. Figure 25 shows that the shape, and especially the maximum in the frequency histogram plots of this data for the 0.42% C alloy are essentially independent of reaction time at 735°C. Figure 26 demonstrates that the all-reaction-times data at each temperature in each alloy studied, and also all of the dihedral angle data consolidated into a single plot, yield the same result. The stereological studies previously discussed showed that the most probable true dihedral is the one which occurs most frequently, even under the non-random sectioning conditions used in this investigation. In all cases, the maximum dihedral angle was found to be 100°±5°. Gjostein et al (34) have previously shown that in the same series of Fe-C alloys thermo-mechanically processed in the manner of C. S. Smith (33) so as to ensure that interphase boundary energy is usually no longer a function of boundary orientation yielded an

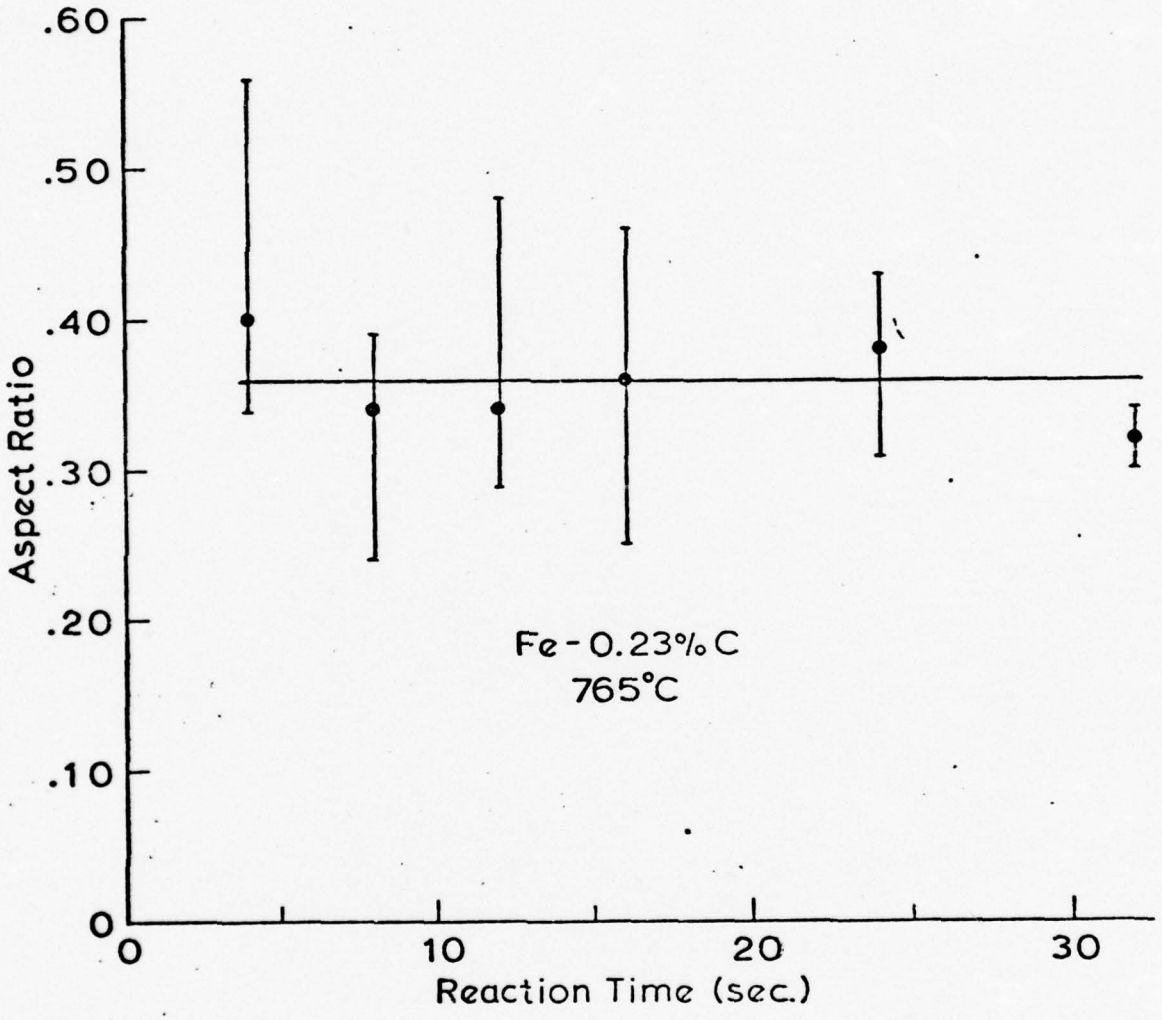
.60
.50
.40
.30
.20
.10
0
Aspect Ratio
Fe - 0.23% C
765°C
0
10
20
30
Reaction Time (sec.)

Figure 22

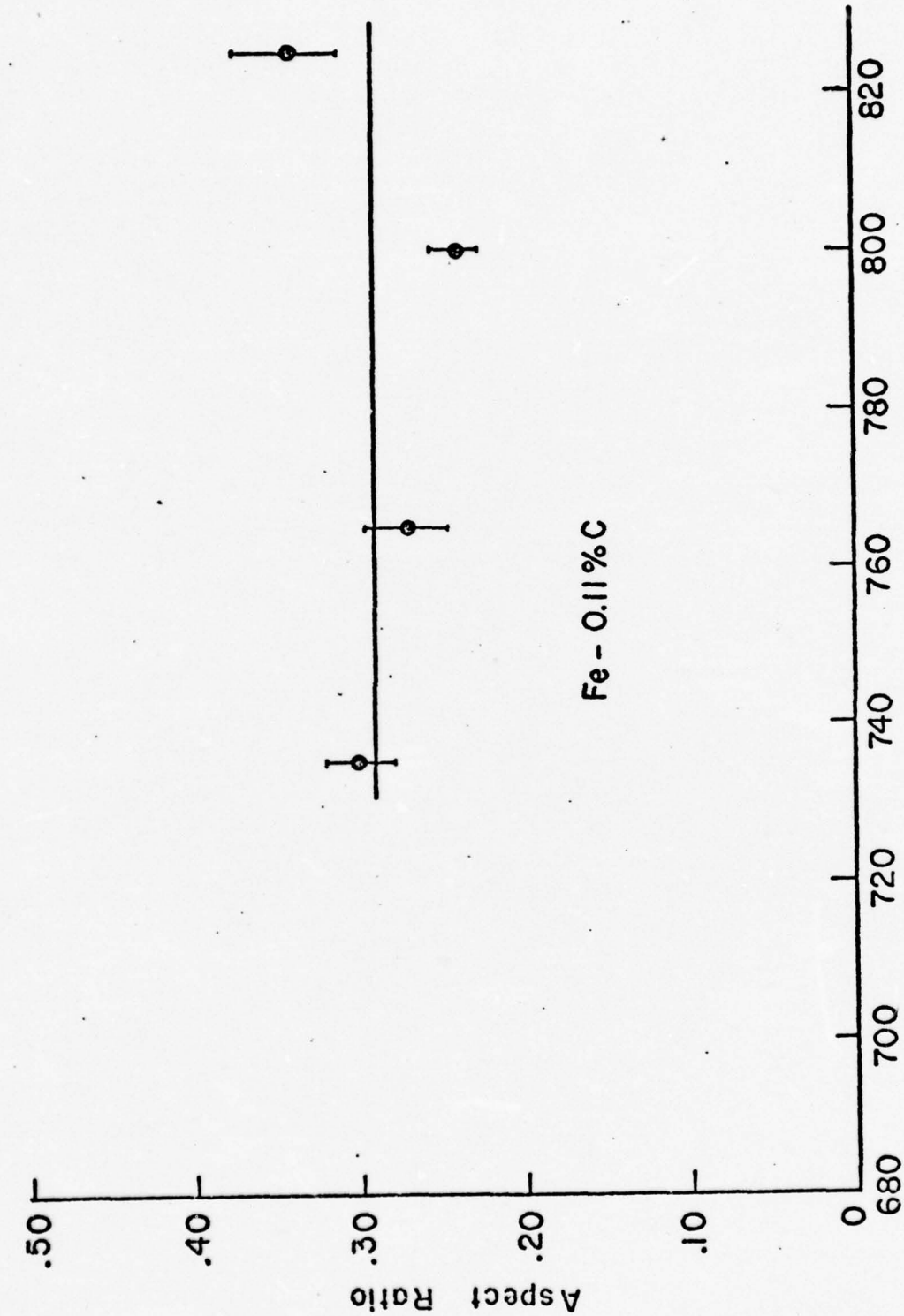
Aspect Ratio
.50
.40
.30
.20
.10
0
680
700
720
740
760
780
800
820
Reaction Temperature, °C
Fe - 0.11% C

Figure 23

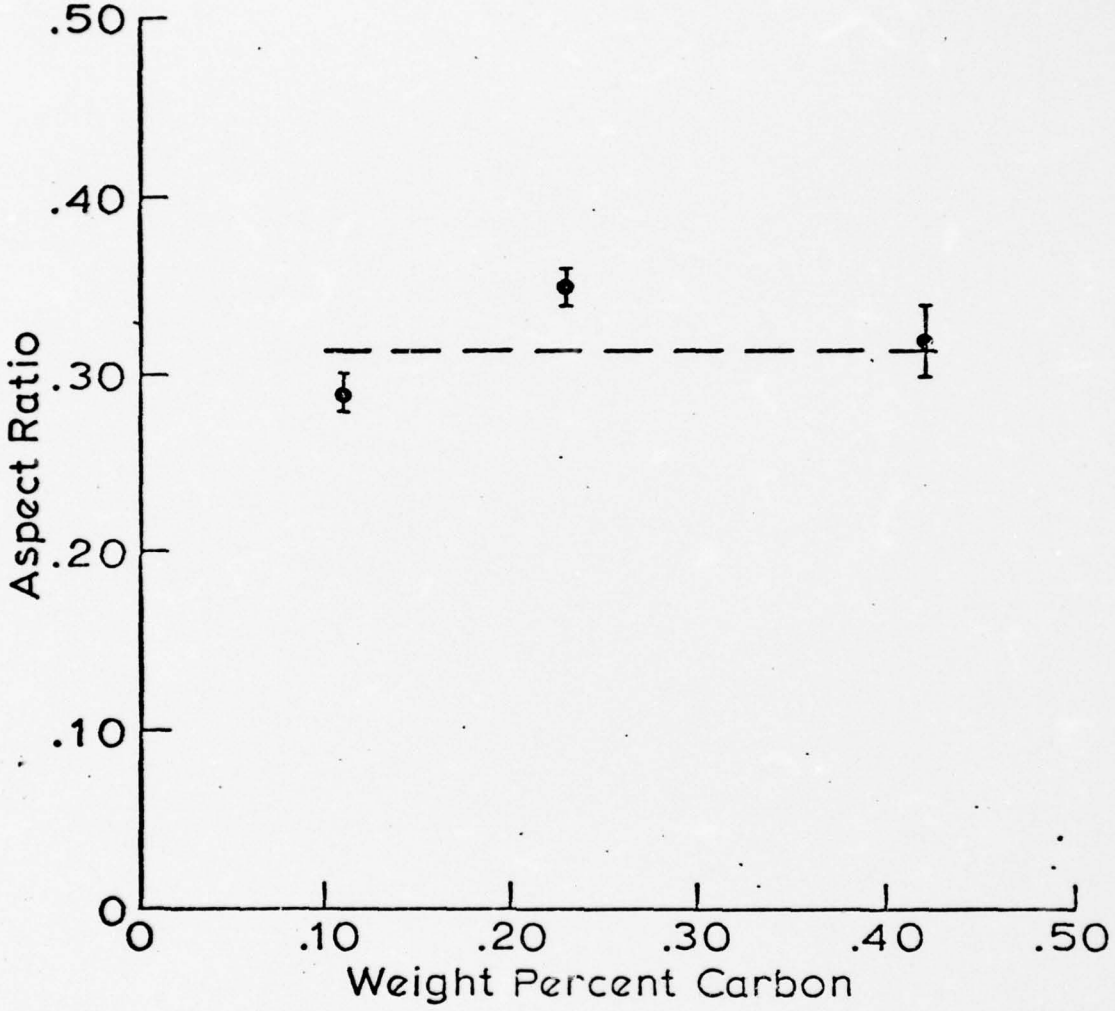
.50
.40
.30
.20
.10
0
Aspect Ratio
0
.10
.20
.30
.40
.50
Weight Percent Carbon

Figure 24

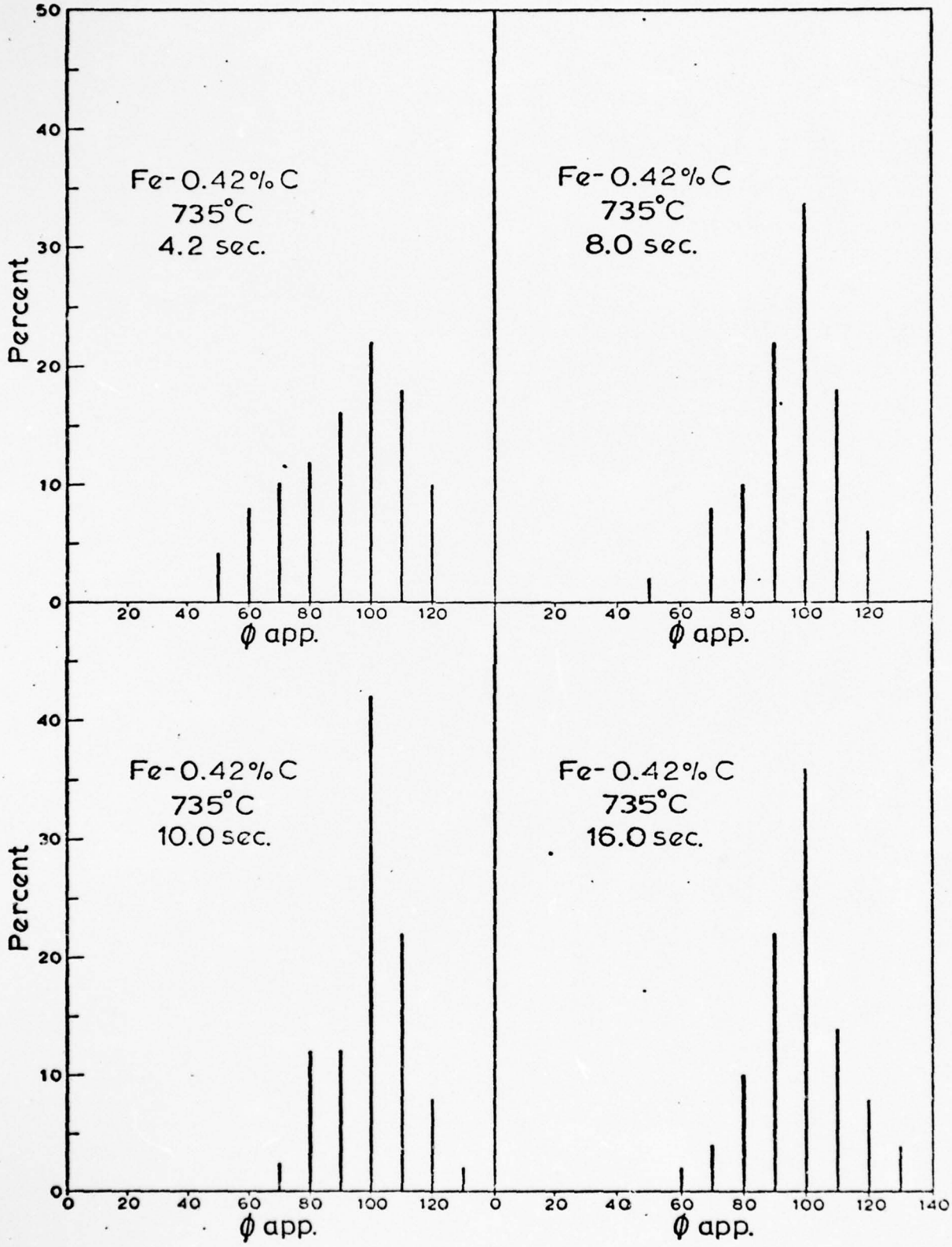
Fe-0.42% C
735°C
4.2 sec.
Fe-0.42% C
735°C
8.0 sec.
Fe-0.42% C
735°C
10.0 sec.
Fe-0.42% C
735°C
16.0 sec.
Percent
φ app.
0
10
20
30
40
50
60
80
100
120
140

Figure 25

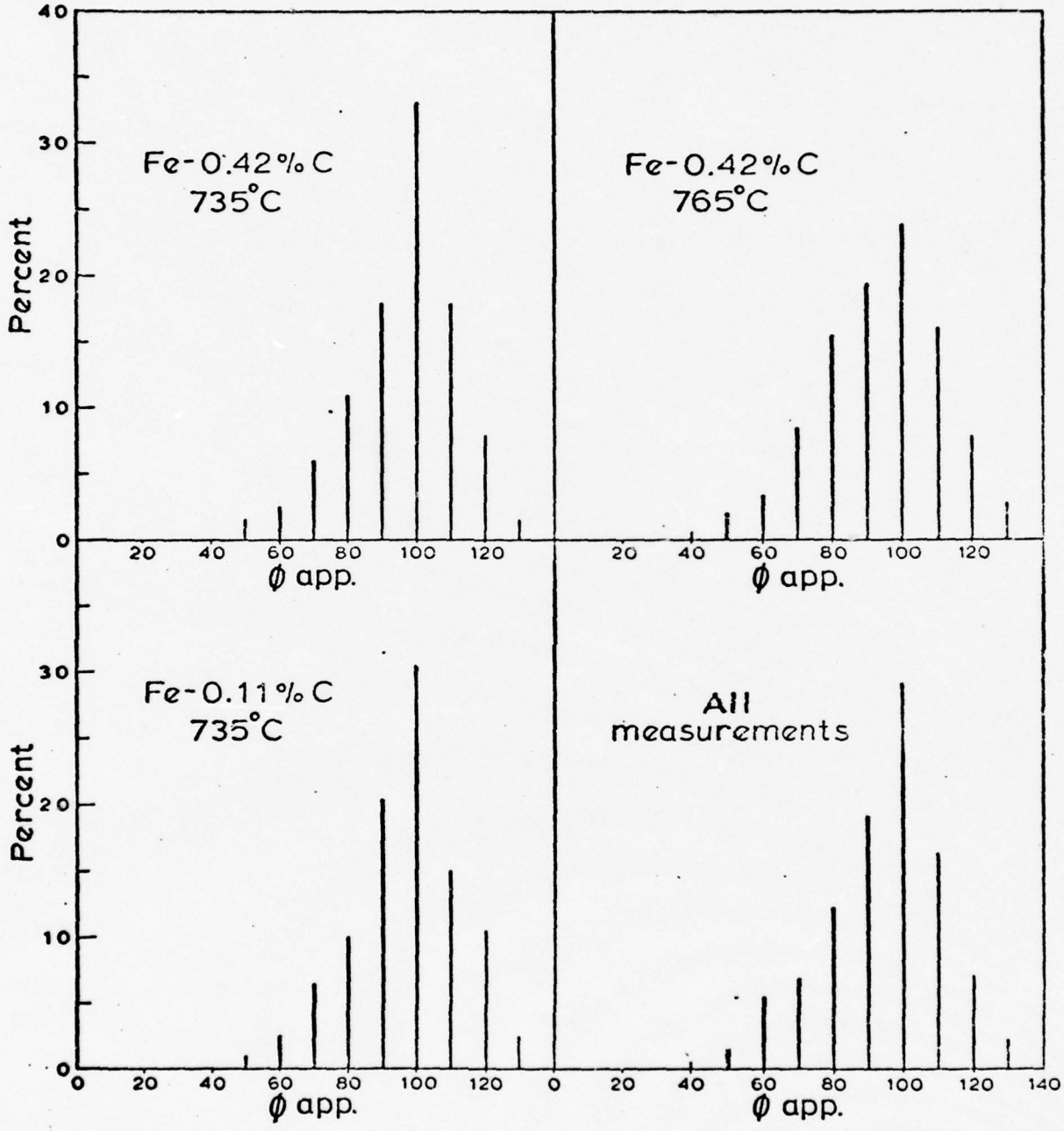
Fe-0.42% C
735°C
Fe-0.42% C
765°C
Fe-0.11% C
735°C
All
measurements
Percent
φ app.
0
10
20
30
40
60
80
100
120
140

Figure 26

equilibrium dihedral angle of 115°. A similar deviation has been reported for grain boundary allotriomorphs of θ phase in an Al-4% Cu alloy (35). Since the growth of ferrite allotriomorphs is essentially controlled by the volume diffusion of carbon in austenite, but slowed down by faceting, whereas θ allotriomorphs have been shown to grow by a grain and interphase boundary diffusion-assisted mechanism (36), it appears that such deviations from equilibrium shape cannot be ascribed to the basic mechanism of growth. A possible alternate explanation is that maximization of the rate of volume increase of an allotriomorph exerts "pressure" on the dihedral angle to make it smaller. The countervailing pressure of interfacial energy minimization near the root of the dihedral angle prevents this angle from approaching zero, and instead results in a compromise angle somewhat smaller than the equilibrium one.

The aspect ratio corresponding to the equilibrium dihedral angle is 0.55 and the ratio given by the dihedral angle during growth is 0.47. The difference between the latter ratio and the one observed experimentally, ca. 1/3, appears to result from faceting on the broad faces of the allotriomorphs.

C. Supplementary Studies

These studies are related in diverse ways to the central themes of the Grant. In many cases, they were either completed in a relatively short period of time, or in the cases of nos. 4 and 13, the extended experimental studies involved were undertaken at another laboratory. Only those studies are reported which appear in the publication list (section II-A of p. 3); they are briefly summarized here in the same order.

1. Relative Growth Kinetics of Ledged and Disordered Interphase Boundaries (with C. Atkinson and K. R. Kinsman)

Experimental results on plate thickening kinetics previously published for several alloy systems have shown, unexpectedly, that the partially or fully coherent broad faces of these plates can sometimes migrate more rapidly than disordered boundaries under the same conditions of reaciton temperature and composition. Using the Jones-Trivedi (37) equation for ledge growth, it was shown that this result is theoretically sound (it has been questioned by some on the ground that excessive solute trans-

port rates might be required), and the conditions under which it should develop are described. Such rapid growth kinetics of ledged boundaries obtain only when the ledges are closely spaced and when the solute diffusion fields associated with adjacent ledges do not seriously overlap. These conditions are particularly well fulfilled during the proeutectoid ferrite reaction in Fe-C alloys because ledges develop readily and the composition difference between austenite and ferrite is relatively small.

2. The Nature of the Barrier to Growth at Partially Coherent FCC:BCC Boundaries (with K. C. Russell, M. G. Hall and K. R. Kinsman)

Hall, Aaronson and Kinsman (6) have deduced that the structure of partially coherent boundaries on b.c.c. Cr plates precipitated from an f.c.c. Cu-Cr matrix consists of effectively coherent regions separated by disordered areas. In this study, two mechanisms through which such an interfacial structure might act as the barrier to growth which the presence of facets during growth requires are considered. In one, it is noted that the coherent areas are so closely spaced that capillarity may halt bulging out of the disordered regions of the boundary between these areas. Calculation shows that this suggestion is feasible for proeutectoid ferrite plates (assumed to have the same interfacial structure on their broad faces as Cr plates), but is appropriate for Cr plates only at relatively small undercoolings below the solvus temperature. The second mechanism considered is that the supposedly disordered regions between the coherent ones may be converted into partially coherent areas by the insertion of a misfit dislocation along the center of each.

Subsequent research, recounted in section II-C of page 3, has shown both experimentally and through modeling that the second suggestion is correct in the case of proeutectoid ferrite plates. It remains possible that the first suggestion may prove applicable in some other alloy system, or perhaps in a transformation involving a still more disparate pair of crystal structures than f.c.c. and b.c.c.

3. On the Driving Force for the Growth of Grain Boundary Allotriomorphs by the "Collector Plate" Mechanism (with K. C. Russell)

Recent experimental evidence indicates that at temperatures below ca.

$0.9T_m$, grain boundary allotriomorphs grow (36,38-40) and dissolve (41,42) by the collector plate mechanism when the matrix is a f.c.c. substitutional solid solution. On this mechanism, atomic transport proceeds via volume diffusion to the grain boundaries, diffusion along these boundaries to the edges of the allotriomorphs and then diffusion along the broad faces of the allotriomorphs (which tend to have a predominantly disordered structure) and deposition on these faces as well as at the edges. This mechanism contrasts with the classical one of volume diffusion directly toward or away from the grain boundary allotriomorphs. The present study sought the common driving force, applicable to both growth and dissolution, for the key element in the collector plate mechanism, namely, diffusion along the interphase boundaries of the allotriomorphs. This driving force was concluded to be departure of the allotriomorphs from equilibrium shape. In the case where the flux of solute along the interphase boundaries is much less than that along the grain boundaries, these departures were deduced to be quite marked. During dissolution, the allotriomorphs become more prolate than at equilibrium, whereas during growth they become more oblate. These departures provide the needed solute concentration gradient toward or away from, respectively, the edges of the allotriomorphs. When the solute flux is more rapid along the interphase boundaries than along the grain boundaries, however, the departures from equilibrium shape must be very small; their directions are not clear, and they will doubtless be very difficult to detect experimentally. Application of this analysis to be published experimental data on the dihedral angles of θ allotriomorphs in Al-4% Cu during growth and at equilibrium (35) indicates that the flux of Cu is significantly more rapid along grain boundaries than along interphase boundaries in this alloy.

4. Thickening Kinetics of Proeutectoid Ferrite Plates in Fe-C Alloys (with K. R. Kinsman and E. Eichen)

The extensive thermionic emission microscopy studies which formed the core of this investigation were carried out while the P.I. was with the Scientific Research Staff of Ford Motor Co. A substantial fraction of the interpretation and manuscript preparation was done after the P.I. had moved to Michigan Tech and was supported

by the present Grant.

The thickening kinetics of proeutectoid ferrite sideplates in Fe-C alloys were measured as a function of reaction temperature and carbon content from motion picture films exposed during the growth of the sideplates. During the first few seconds of growth, the thickening rate is $5 \times 10^{-5\pm1}$ cm./sec.; afterwards it usually diminishes to $1 - 30 \times 10^{-6}$ cm./sec. Variations in kinetics at a given temperature in a particular alloy are virtually as large as those encompassed by the entire range of carbon content (0.11 to 0.42%) and reaction temperature (up to ca. 100°C) investigated. As predicted by a general theory of precipitate morphology (1,2), thickening was shown to occur only by the ledge mechanism. The lengthening rate of particularly large ledges was measured and was found to be approximately that allowed by the diffusion of carbon in austenite. Ledge heights and spacings between ledges were measured, primarily with replication electron microscopy, and were found to range from hundreds to tenths of a micron and from tenths to nearly ten microns, respectively. At early stages of reaction, the range of ledge spacings calculated from the measured thickening kinetics agreed with that directly measured. At later reaction times, however, the calculated spacings were about an order of magnitude too large, indicating that most of the ledges acquire a partially coherent structure at their edges during the later stages of growth and are thereby virtually inactivated. Tent-shaped and more complex surface relief effects were observed; invariant plane strain reliefs, characteristics of a martensitic transformation, were only rarely found. These features are readily explained in terms of a diffusional transformation taking place by means of the ledge mechanism.

(These results, it should also be noted, are consistent with the findings of the present investigation on the structure of the broad faces of ferrite plates, as described in section II-C of page 3.)

5. Observations on Interphase Boundary Structure

This was an invited review paper, presented at a symposium on Interfaces held by the Royal Microscopical Society in London and published shortly thereafter in

The Journal of Microscopy. Emphasis was placed upon observations reported since 1968, when a previous review paper on this subject (and on the growth mechanisms of interphase boundaries) was prepared (2).

Nearly all of the boundaries considered were of the partially or fully coherent type, and hence the principal structural features examined were misfit dislocations and ledges. Observations were drawn from studies of precipitation, spinodal decomposition, oriented overgrowth and eutectics. Interphase boundary structures were found to be little affected in the main by the type of reaction through which they were developed and were consistent with van der Merwe theory (43,44) and with a general theory of precipitate morphology (1,2). Observations of these structures have been considerably facilitated by the efforts of Weatherly and co-workers (45-47) to define the visibility and optimum TEM viewing conditions of misfit dislocations and ledges. (These results are already becoming obsolescent as a result of the weak-beam, dark-field technique developed by Cockayne (8); both the misfit dislocations and the ledges described in section II-C of page 3 are more closely spaced than the minimum resolution limits estimated by Weatherly and his colleagues. It should be noted, though, that Weatherly et al did forecast this development.) Important new observations made on misfit dislocations since 1968 include: misfit dislocation spacings in the Cr(mo)/NiAl eutectic are in good agreement with theoretical expectation because misfit dislocations are also glide dislocations and the interface plane is also the glide plane (48); misfit dislocations on θ' Al-Cu and η Al-Au plates with a Burgers vector ($\underline{a}/2\langle 100\rangle$) stable only at an interphase boundary (49); reduction of the interfacial energy of partially coherent boundaries on the same precipitates by dislocation interactions and rearrangements (49); reduction of interfacial energy of interfaces developed during spinodal decomposition through rotation of the interface itself from {100} to {110} (50); and misfit dislocation boundaries between f.c.c. (Cu-rich) and b.c.c. (Cr) crystals made possible with the assistance of "structural ledges" (6). Growth ledges have now been observed in a number of alloy systems which have undergone precipitation from solid solution or eutectic solidification; they appear to be confirmed as a customary feature of

migrating partially or fully coherent interphase boundaries. Much new experimental information has been obtained on the sources (exceedingly diverse), heights (usually appreciably higher than monatomic), spacings (irregular) and migration kinetics (diffusion-controlled if their edges are disordered) of ledges. New observations continue to confirm the complexity of the processes through which misfit dislocations are acquired. The Ashby-Johnson (51) and the Brown-Woolhouse (52) theories of misfit dislocation nucleation or acquisition by spherical precipitates are in encouraging agreement with experiment.

6. Influence of Alloying Elements upon the Morphology of Austenite Formed from Martensite in Fe-C-X Alloys (with M. R. Plichta)

Using a modification of the boiling alkaline sodium picrate etching technique (53) and high-purity Fe-C-X alloys, systematic effects of alloying elements upon the later reaction time microstructure generated during the formation of austenite from martensite in the $\alpha + \gamma$ region were observed. At early stages of reaction, the microstructure was qualitatively similar in all of the alloys investigated: grain boundary allotriomorphs and idiomorphs at the former austenite grain boundaries and martensite needle boundary (MNB) allotriomorphs in the interiors of the former austenite grains. At later reaction times, however, the microstructure of Fe-C, Fe-C-Mo and Fe-C-Cr alloys consisted of allotriomorphs and idiomorphs at the former austenite grain boundaries but only idiomorphs in the interiors of the grains. The ferrite grain structure had become coarsely equiaxed. In Fe-C-Mn, Fe-C-Ni and Fe-C-Cu alloys, on the other hand, the initial microstructure was largely unchanged and the ferrite grain boundaries exhibited an acicular pattern strongly reminiscent of its martensitic antecedent. In Fe-C-Si, Fe-C-Al and Fe-C-Co alloys, the microstructure was like that of the Mn, Ni and Cu alloys only where differently oriented packets of martensite had met, and otherwise closely resembled that of the Fe-C, etc. group of alloys. These results were explained in terms of competition between the rates of nucleation of austenite at the various boundaries in the martensitic starting structure and the migration of the original martensite:martensite boundaries into lower energy configurations.

7. Analysis of the Composition of α_1 Plates Precipitated from β' Cu-Zn Using Analytical Electron Microscopy (with G. W. Lorimer, G. Cliff and K. R. Kinsman)

The composition of α_1 plates in a Cu-40.5% Zn alloy isothermally reacted at 335°C was determined as a function of reaction time by means of an analyzing electron microscope, EMMA-4. This instrument is capable of determining accurately the composition of crystals whose minimum dimension is as small as 500-1000 Å. At all stages of growth which could be studied with this instrument, the Zn content of the α_1 plates is markedly less than that of the β' matrix. Thus, despite the fact that these plates have been shown to exhibit the crystallography, surface relief effect and internal structure characteristic of martensite (54), they must have formed by a diffusional growth mechanism, rather than by one of shear. This finding supports the view (1,2) that the crystallography and surface relief effects characteristic of martensite are a necessary but not a sufficient condition for identification of the reaction mechanism as one of shear.

The experimental results obtained during this study directly contradict those of Cornelis and Wayman (55), obtained with a different instrument. We have suggested this conflict arose because Cornelis and Wayman used an instrument operated at 40 kV, whereas EMMA-4 was employed at 100 kV; the lower operating voltage appears to give rise to excessive diffusion of electrons, thereby markedly increasing the effective measurement spot diameter. Hence, at early reaction times the measurements evidently included not only the thickness of the α_1 plates but also enough of the β' matrix so that the instrument did not register any change in average composition.

This argument is a crucial one in the diffusional growth vs. shear controversy, because all of the crystallographic and surface relief effect evidence indicates that α_1 plates could have formed by shear; only the nonfulfillment of the one remaining specification of the phenomenological theory of martensite, namely, that there be initially no composition difference between matrix and product phases, indicates that α_1 plates form by a diffusional growth mechanism. As Wayman (56) had clearly noted, all

of the specifications of the phenomenological theory must be fulfilled in order that the transformation product be describable as martensite. Since the α_1 Cu-Zn transformation is the only reaction which seems to provide, at the present time, an agreed upon testing ground for the basic controversy, the disagreement over experimental results has not been ended by the publication of our contribution. Item no. 11 presents a reply to a published argument against our experimental results. Wayman privately indicates that he is conducting further experimental work on the problem and expects to publish his new results soon. Kinsman et al (57) have repeated our measurements using an instrument of the type employed by Cornelis and Wayman (newly installed at the Ford Laboratories) and have concluded that this instrument does indeed have less than the advertised spatial resolution, but that, given careful adjustment, it still yields results qualitatively the same as we have reported, namely, that α_1 differs in composition from its matrix even at the earliest accessible reaction times. But it is not unlikely that several exchanges in the literature will be required before a generally acceptable conclusion to the argument over the experimental results is reached.

8. The Watson-McDougall Shear: Proof That Widmanstatten Ferrite Cannot Grow Martensitically (with M. G. Hall, D. M. Barnett and K. R. Kinsman)

Watson and McDougall (23) observed experimentally that tent-shaped and invariant plane strain surface reliefs produced by proeutectoid ferrite plates in an Fe-C alloy correspond to an average transformation shear strain of 0.36. Combining a standard statistical thermodynamic treatment of free energy changes associated with the austenite-to-ferrite transformation (58), Eshelby's (59) equation for shear strain energy as a function of aspect ratio and measurements on the micrographs of Watson and McDougall of the aspect ratio of ferrite plates, it was shown that the formation of ferrite plates with the Watson-McDougall shear is thermodynamically impossible effectively through the temperature-composition region of the proeutectoid ferrite reaction. This result obtains whether the ferrite plates contain the metastable equilibrium carbon content corresponding to the shear strain energy-depressed Ae3 or fully inherit the

carbon content of the parent austenite.

A critical examination of the crystallographic results reported by Watson and McDougall shows poor agreement with the phenomenological theory of martensite. Also, the surface relief effects associated with proeutectoid ferrite plates are pointed out to be only rarely of the invariant plane strain morphology (see II-D-4 of p. 3), the only type of relief to which the phenomenological theory can be applied.

These considerations provide, in sum, further support for our view that shear plays no role at all in the formation of proeutectoid ferrite plates.

9. Considerations on a Martensitic Mechanism for the F.C.C.→B.C.C. Transformation in a Cu-0.33 W/O Cr Alloy (with M. G. Hall and G. W. Lorimer)

A previous investigation by Hall et al (6) showed that Cr precipitate plates in a Cu-0.33 W/O Cr alloy usually have an irrational habit plane and can have irrational lattice orientation relationships as well. These are characteristics customarily ascribed to the product of a martensitic transformation. The present study was undertaken to ascertain whether or not these Cr precipitates exhibit the other characteristics of martensite.

Surface relief effects of Cr plates which nucleated below and grew into the specimen surface were found to be tent-shaped, rather than of the invariant plane strain morphology characteristic of martensite. Analysis of Cr precipitates during early stages of growth by means of EMMA-4 showed that the precipitates contain distinctly more Cr than the matrix, again in contradistinction to the absence of a composition change required of a martensitic transformation. Upon the basis of the Crocker-Bilby (60) version of the phenomenological theory of martensite, the habit planes predicted for Cr precipitates on the criteria of minimum shear, minimum Burgers vector of surface dislocation and physically operative deformation modes in either phase for the lattice invariant deformation were compared with those experimentally observed. Each criterion was able to account for no more than a few of the observed habit planes; explaining all of them on a martensitic basis results in the physically implausible requirement that

a variety of lattice invariant deformation mechanisms be simultaneously operative. All of the foregoing contradictions are readily resolved, however, if it is accepted that Cr plates form entirely by a nucleation and diffusional growth mechanisms.

These results encouraged an empirical comparison of the habit planes of Cr plates in Cu-Cr with those of ferrite, bainite and martensite in steel. It was noted that Cr, ferrite and bainite plates, all of which we believe form by nucleation and diffusional growth, have habit planes in different areas of the stereographic triangle than those of martensite.

10. Application of a Rapid Chemical Polish to Preparation of High-Carbon Steel Specimens for Optical Microscopy (with M. R. Plichta and W. F. Lange III)

The usefulness of a HF-H_2O_2-H_2O chemical polish for the preparation of optical microscopy-quality polishes on steel specimens has been explored as a function of microstructure. Both Fe-C and Fe-C-X alloys were used in this study. Good results were readily obtained on entirely martensitic and on martensite + ferrite microstructures, though excessively rapid attack sometimes occurred on certain grain and interphase boundaries. Chemical polishing of pearlite was found to be more difficult because of severe attack on ferrite:carbide boundaries. Very short polishing times (ca. 4 secs.) are required in order to avoid destroying the definition of the carbide lamellae. This polish was judged to be useful because of the ease and simplicity of its use, but to require a considerable measure of caution if high quality results are to be achieved.

11. Reply to "Comments on 'Analysis of the Composition of α_1 Plates Precipitated from β' Cu-Zn Using Analytical Electron Microscopy" (with G. W. Lorimer, G. Cliff and K. R. Kinsman)

This is a reply to a discussion, presented by M. M. Kostic and E. B. Hawbolt, to item II-D-7. These writers suggested that since our measurements were made on the α_1 plates which protruded out of the β' matrix (as a result of preferential electro-polishing), the plates were heated during electron probe counting sufficiently for their Zn content to be preferentially boiled away. During the present study, this

hypothesis was tested by incrementally counting the α_1 plates at a fixed position over a wide range of counting times. The ratio of the counting rate of Cu to that of Zn (using the K_α radiation of both) was found to be independent of counting time, thereby refuting the suggestion of Kostic and Hawbolt.

12. A Critical Test of Two Theories of Non-IPS Geometric Surface Relief Effects Associated with Diffusional Phase Transformations (with K. R. Kinsman)

θ Al-Cu rods have been previously shown to develop tent- or vee-shaped surface relief effects (61,62). It has been proposed that these effects are produced by ledgewise growth which establishes the shape change through maintenance of partial coherency across the broad faces of the ledges; the actual rod thickening process is suggested to take place at the edges of the ledges through diffusional jumps across these disordered interphase boundaries (2,61,63). Clark and Wayman (62) have suggested that the tent-shaped reliefs are the result of an anisotropic (bulk) volume change accompanying the transformation. The present study was undertaken to distinguish critically between the two theories. Surface relief observations were made on grain boundary allotriomorphs of θ in an Al-4% Cu alloy by means of interference and replication electron microscopy. Negligible surface relief effects were observed. This is consistent with the former mechanism, since thickening of grain boundary allotriomorphs does not proceed primarily by the ledge mechanism. However, this result is inconsistent with the Clark-Wayman mechanism, which ought to function irrespective of the type of interfacial structure present.

13. Growth Mechanisms of AuCu II Plates (with K. R. Kinsman)

A joint investigation of this topic was undertaken with Drs. J. Kittl and A. Pedraza of the Buenos Aires laboratories of the Argentine Atomic Energy Commission; the experimental work was performed largely in Buenos Aires; Dr. Kinsman and the P.I. visited Argentina (while the P.I. was still with the Ford laboratories) to participate directly in this investigation, and subsequently continued their involvement by

mail. When the investigation was recently completed, after a number of delays, it was found that the U. S. and the Argentinian authors were unable to agree on a common interpretation. Accordingly, each prepared separate papers for submission to Acta Metallurgica based upon the same set of results. The brief summary of our views given here actually conflicts surprisingly little with those of the Argentinians; we have ended up emphasizing different aspects of the problem and have thus in good part written complementary rather than opposed papers.

The lengthening and thickening rates of AuCu II plates measured by Pedraza and Kittl are used as a basis for understanding the mechanisms through which these rates develop. These rates are 3-4 orders of magnitude smaller than those estimated for incoherent AuCu II:disordered matrix (interphase) boundaries. During growth, the interphase boundaries are deduced to be coherent. At the edges of plates, coherency is maintained because the succession of ledges is too rapid to give the misfit dislocation structure time to develop. At the broad faces of plates, the closely spaced twins (initially, ca. 50 Å apart (64)) in the AuCu II greatly diminish the driving force for introduction of misfit dislocations until substantial coarsening of the twinned structure has occurred. Ledge growth at the broad faces is inhibited by the requirement that such growth occur parallel to the twins; this effect appears responsible for the order of magnitude larger spacing between ledges at the broad faces than at the edges of the plates and for the growth of AuCu II crystals as plates rather than as idiomorphs. The principal features of AuCu II growth were shown to be consistent with a massive rather than with a martensitic mode of transformation.

D. Publications Resulting in Whole or in Part from Research Supported by This Grant

1. C. Atkinson, K. R. Kinsman and H. I. Aaronson, "Relative Growth Kinetics of Ledged and Disordered Interphase Boundaries," Scripta Met., 7, 1105 (1973).

2. K. C. Russell, M. G. Hall, K. R. Kinsman and H. I. Aaronson, "The Nature of the Barrier to Growth at Partially Coherent FCC:BCC Boundaries," Met. Trans., 5, 1503 (1974).

3. K. C. Russell and H. I. Aaronson, "On the Driving Force for the Growth of Grain Boundary Allotriomorphs by the 'Collector Plate' Mechanism," Scripta Met., 8, 559 (1974).

4. K. R. Kinsman, E. Eichen and H. I. Aaronson, "Thickening Kinetics of Proeutectoid Ferrite Plates in Fe-C Alloys," Met. Trans., 6A, 303 (1975).

5. H. I. Aaronson, "Observations on Interphase Boundary Structure," Jnl. of Microscopy, 102, 275 (1974).

6. M. R. Plichta and H. I. Aaronson, "Influence of Alloying Elements upon the Morphology of Austenite Formed from Martensite in Fe-C-X Alloys," Met. Trans., 5, 2611 (1974).

7. G. W. Lorimer, G. Cliff, H. I. Aaronson and K. R. Kinsman, "Analysis of the Composition of α_1 Plates Precipitated from β' Cu-Zn Using Analytical Electron Microscopy," Scripta Met., 9, 271 (1975).

8. H. I. Aaronson, M. G. Hall, D. M. Barnett and K. R. Kinsman, "The Watson-McDougall Shear: Proof That Widmanstatten Ferrite Cannot Grow Martensitically," Scripta Met., 9, 533 (1975).

9. M. G. Hall, H. I. Aaronson and G. W. Lorimer, "Considerations on a Martensitic Mechanism for the F.C.C.→B.C.C. Transformation in a Cu-0.33 W/O Cr Alloy," Scripta Met., 9, 533 (1975).

10. M. R. Plichta, H. I. Aaronson and W. F. Lange III, "Application of a Rapid Chemical Polish to Preparation of High-Carbon Steel Specimens for Optical Microscopy," Metallography, in press.

11. G. W. Lorimer, G. Cliff, H. I. Aaronson and K. R. Kinsman, "Reply to 'Comments on "Analysis of the Composition of α_1 Plates Precipitated from β' Cu-Zn Using Analytical Electron Microscopy," Scripta Met., 9, 1175 (1975).

12. K. R. Kinsman and H. I. Aaronson, "A Critical Test of Two Theories of Non-IPS Geometric Surface Relief Effects Associated with Diffusional Phase Transformations," Met. Trans., 7A, 896 (1976).

13. H. I. Aaronson and K. R. Kinsman, "Growth Mechanisms of AuCu II Plates," Acta Met., in press.

14. J. R. Bradley and H. I. Aaronson, "The Stereology of Grain Boundary Allotriomorphs," Met. Trans., in press.

15. J. R. Bradley, J. M. Rigsbee and H. I. Aaronson, "Growth Kinetics of Grain Boundary Ferrite Allotriomorphs," Met. Trans., in press.

5. Bibliography

1. H. I. Aaronson, "Decomposition of Austenite by Diffusional Processes," p. 387, Interscience, New York (1962).

2. H. I. Aaronson, C. Laird and K. R. Kinsman, "Phase Transformations," p. 313, ASM, Metals Park, OH (1970).

3. H. I. Aaronson, Jnl. of Microscopy, 102, 275 (1974).

4. H. Brooks, "Metals Interfaces," p. 20, ASM, Metals Park, OH (1952).

5. H. W. Paxton, Jnl. Chem. Phys., 26, 1769 (1957).

6. M. G. Hall, H. I. Aaronson and K. R. Kinsman, Surface Science, 31, 257 (1972).

7. K. C. Russell, M. G. Hall, K. R. Kinsman and H. I. Aaronson, Met. Trans., 5, 1503 (1974).

8. D. J. H. Cockayne, Jnl. of Microscopy, 98, 116 (1973).

9. T. B. Massalski, "Phase Transformations," p. 433, ASM, Metals Park, OH (1970).

10. E. B. Hawbolt and T. B. Massalski, Met. Trans., 1, 2315 (1970).

11. M. R. Plichta, J. M. Rigsbee, M. G. Hall, K. C. Russell and H. I. Aaronson, Scripta Met., in press.

12. R. W. Heckel and H. W. Paxton, Trans. ASM, 53, 539 (1961).

13. R. F. Mehl, C. S. Barrett and D. W. Smith, Trans. AIME, 105, 215 (1933).

14. A. B. Greninger and A. R. Troiano, ibid, 140, 307 (1940).

15. R. W. Heckel, J. H. Smith and H. W. Paxton, ibid, 218, 567 (1960).

16. H. I. Aaronson and H. A. Domian, ibid, 236, 781 (1966).

17. P. G. Boswell, K. R. Kinsman and H. I. Aaronson, unpublished research.

18. R. W. K. Honeycombe, Met. Trans., 3, 1099 (1972).

19. R. W. K. Honeycombe, Met. Trans., to be published (IMD Lesture, Las Vegas Meeting of TMS, 1976).

20. G. V. Kurdjumow and G. Sachs, Z. Physik, 64, 325 (1939).

21. Z. Nishiyama, Sci. Rept. Tohoku Univ., 23, 368 (1934).

22. G. Wasserman, Arch. Eisenhüttenwesen, 16, 647 (1933).

23. J. D. Watson and P. G. McDougall, Acta Met., 21, 961 (1973).

24. H. I. Aaronson, M. G. Hall, D. M. Barnett and K. R. Kinsman, Scripta Met., 9, 705 (1975).

25. H. Gleiter, Acta Met., 17, 565 (1969).

26. K. R. Kinsman and H. I. Aaronson, "Transformation and Hardenability in Steels," Climax Molybdenum Co., p. 39, Climax Molybdenum Co., Ann Arbor, MI (1967).

27. C. Atkinson, K. R. Kinsman, H. B. Aarons and H. I. Aaronson, Met. Trans., 4, 783 (1973).

28. K. R. Kinsman and H. I. Aaronson, ibid, 4, 959 (1973).

29. R. T. DeHoff, Met. Trans., 2, 521 (1971).

30. G. Horvay and J. W. Cahn, Acta Met., 9, 695 (1961).

31. C. Atkinson, Trans. AIME, 245, 801 (1969).

32. D. E. Coates, Met. Trans., 4, 2313 (1973).

33. C. S. Smith, Trans. AIME, 175, 15 (1948).

34. N. A. Gjostein, H. A. Domian, H. I. Aaronson and E. Eichen, Acta Met., 14, 1637 (1966).

35. H. B. Aaron and H. I. Aaronson, ibid, 18, 699 (1970).

36. H. B. Aaron and H. I. Aaronson, ibid, 16, 789 (1968).

37. G. J. Jones and R. K. Trivedi, Jnl. App. Phys., 42, 4299 (1971).

38. J. Goldman, H. I. Aaronson and H. B. Aaron, Met. Trans., 1, 1805 (1970).

39. A. D. Brailsford and H. B. Aaron, 40, 1702 (1969).

40. E. B. Hawbolt and L. C. Brown, Trans. AIME, 239, 1916 (1967).

41. A. Pasparakis, D. E. Coates and L. C. Brown, Acta Met., 21, 991 (1973).

42. A. Pasparakis and L. C. Brown, ibid, 21, 1259 (1973).

43. J. H. Van der Merwe, Jnl. App. Phys., 34, 117 (1963).

44. J. H. Van der Merwe, ibid, 34, 123 (1963).

45. G. C. Weatherly, Acta Met., 19, 181 (1971).

46. G. C. Weatherly and C. M. Sargent, Phil. Mag., 22, 1049 (1970).

47. G. C. Weatherly and T. D. Mok, Surface Science, 31, 335 (1972).

48. H. E. Cline, J. L. Walter, E. F. Koch and L. M. Osika, Acta Met., 19, 405 (1971).

49. R. Sankaran and C. Laird, Phil Mag., 29, 179 (1974).

50. R. J. Livak and G. Thomas, Acta Met., 22, 589 (1974).

51. M. F. Ashby and L. Johnson, Phil. Mag., 20, 1009 (1969).

52. L. M. Brown and G. R. Woolhouse, Phil. Mag., 21, 329 (1970).

53. H. I. Aaronson, T. L. Johnston and D. J. Schmatz, Trans. ASM, 61, 349 (1968).

54. I. Cornelis and C. M. Wayman, Acta Met., 22, 301 (1974).

55. I. Cornelis and C. M. Wayman, Scripta Met., 7, 759 (1973).

56. H. McI. Clark and C. M. Wayman, "Phase Transformations," p. 59, ASM, Metals Park, OH (1970).

57. K. R. Kinsman, R. H. Richman and J. D. Verhoeven, unpublished research.

58. L. Kaufman, S. V. Radcliffe and M. Cohen, "Decomposition of Austenite by Diffusional Processes," p. 313, Interscience, New York (1962).

59. J. D. Eshelby, Proc. Roy. Soc., 241A, 376 (1957).

60. A. G. Crocker and B. A. Bilby, Acta Met., 9, 678 (1961).

61. K. R. Kinsman, H. I. Aaronson and C. Laird, ibid, 15, 1244 (1967).

62. H. McI. Clark and C. M. Wayman, Met. Trans., 3, 1979 (1972).

63. K. R. Kinsman, E. Eichen and H. I. Aaronson, ibid, 6A, 303 (1975).

64. A. M. Hunt and D. W. Pashley, Jnl. Australian Inst. Metals, 8, 61 (1963).